# Partial Unfolding of Dodecameric Glutamine Synthetase from *Escherichia coli*: Temperature-Induced, Reversible Transitions of Two Domains†

Andrew Shrake,‡ Mark T. Fisher,§,‖ Patrick J. McFarland,§,⊥ and Ann Ginsburg*,§

*Section on Protein Chemistry, Laboratory of Biochemistry, National Heart, Lung, and Blood Institute, National Institutes of Health, Bethesda, Maryland 20892, and Division of Blood and Blood Products, Center for Biologics Evaluation and Research, Food and Drug Administration, Bethesda, Maryland 20892*

*Received December 29, 1988; Revised Manuscript Received March 28, 1989*

ABSTRACT: Glutamine synthetase (GS), $M_r$ 622 000, from *Escherichia coli* contains 12 active sites formed at heterologous interfaces between subunits [Almassy, R. J., Janson, C. A., Hamlin, R., Xuong, N.-H., & Eisenberg, D. (1986) *Nature (London) 323*, 304–309]. Temperature-induced changes in UV spectra from 3 to 68 °C were reversible with the $Mn^{2+}$– or $Mg^{2+}$–enzyme at pH 7.0 (50 °C) in 100 mM KCl. No dissociation or aggregation of dodecamer occurred at high temperatures. The thermal transition involves the exposure of ~0.7 of the 2 Trp residues/subunit (by UV difference spectroscopy) and 2 of the 17 Tyr residues/subunit (change in exposure from 4.7 to 6.7 Tyr/subunit by second-derivative spectral analysis). Monitoring changes in Trp and Tyr exposure independently gives data that conform to a two-state model for partial unfolding with $T_m$ values (where $\Delta G_{unfolding} = 0$) differing by 2–3 °C at each level of $[Mn^{2+}]$ studied and with average $\Delta H_{vH}$ values of 80 and 94 kcal/mol, respectively. These observations suggest that two regions of the oligomeric structure unfold separately as independent transitions (random model). However, the data can be fit equally well with a sequential model in which the Trp transition occurs first upon heating. By fitting with either model, $T_m$ values increase from ~47 to ~54 °C with increasing free $[Mn^{2+}]$ from 3.6 to 49 μM but decrease from ~54 to ~43 °C by further increasing free $[Mn^{2+}]$ from 0.05 to 10 mM; such behavior indicates that the high-temperature form of the enzyme binds $Mn^{2+}$ more weakly but has more binding sites than the native enzyme. The high-temperature Mn·enzyme form is somewhat less unfolded than is the catalytically inactive apoenzyme, which undergoes no further Trp or Tyr exposure on heating and therefore is assumed to be the high-temperature form of divalent cation–free GS. Adding substrates [ADP, L-Met-(*SR*)-sulfoximine, Gln, Gln + $NH_2OH$, or Gln + ADP] to Mn·GS increased $T_m$ to varying extents by preferential binding to the folded form. Indeed, the transition-state analogue complex GS·$(Mn_2$·ADP·L-Met-(*S*)-sulfoximine phosphate$)_{12}$ was stable in the folded form to at least 72 °C. Moreover, an Arrhenius plot for γ-glutamyl transfer activity was linear from 4 to 72 °C with $E_a$ = 18.3 kcal/mol. The temperature dependence of $K_m$ for Gln also was measured from 5 to 72 °C, and a fit of these data gave $\Delta H_{vH}$ = −8.58 kcal/mol, $\Delta C_p$ = −322 cal/(K·mol), and $K_m$ = 1.7 at 37 °C for the binding of Gln to the native enzyme. Thus, the thermally induced transitions of dodecameric Mn·GS appear to involve a loosening of active-site structures, which are stabilized through the free energy of substrate binding.

A goal of studies on protein folding is understanding the stabilization of complex secondary and tertiary structures in native proteins that leads to their unique conformations. Assembly processes and biological interactions depend on the correct folding of polypeptide chains. If an unfolding reaction can be described as a reversible, two-state transition, the thermodynamics of protein folding/unfolding can be determined experimentally from measuring the free energy of unfolding as a function of temperature; $\Delta G$ and changes in other thermodynamic properties then are defined as recently reviewed by Schellman (1987a). Indeed, many small globular proteins unfold in an apparent two-state process (Lumry et al., 1966) on heating (Privalov, 1979) or on adding increasing concentrations of urea or guanidinium salts (Pace, 1975; Schellman, 1987b). In these cases, intermediates are present in sufficiently low concentrations such that they are not detectable in equilibrium measurements (Lumry et al., 1966; Shortle, 1987). In some other cases, the unfolding of separate domains within a protein can be adequately represented by independent two-state processes (Privalov, 1982). Oligomeric proteins may unfold after dissociation of subunits, or unfolding and dissociation may occur concertedly. However, oligomeric proteins often denature irreversibly during heating due to aggregation of dissociated, unfolded subunits. Sturtevant (Manly et al., 1985; Edge et al., 1985) and Mateo (Sãnchez-Ruiz et al., 1988) and their co-workers have demonstrated that an overall irreversible process may be treated as a reversible unfolding reaction if the irreversible aggregation of the unfolded species is slow compared to the rates of interconversion of the native and unfolded species.

High-precision scanning calorimetry (Privalov, 1979, 1982; Sturtevant, 1977) has established that hydrophobic interactions as postulated by Kauzmann (1959) have a dominant role in promoting native protein folding. Hydrophobic interactions arise from increased solvation of unfolded polypeptide chains relative to that of folded forms (Brandts, 1964; Baldwin, 1986). Recently, however, Kauzmann (1987) noted that although exposure of hydrophobic residues can account for the observed

† Presented in part at the 32nd Annual Meeting of the Biophysical Society, February 28–March 3, 1988 (Shrake et al., 1988).

* Address correspondence to this author at NHLBI/NIH, Building 3, Room 208, Bethesda, MD 20892.

‡ Food and Drug Administration.

§ National Institutes of Health.

‖ Staff Fellow, Section on Enzymes, Laboratory of Biochemistry, NHLBI/NIH, Building 3, Room 122, Bethesda, MD 20892.

⊥ Present address: Laboratory of Immunoregulation, NIAID/NIH, Building 10, Room 11B13, Bethesda, MD 20892.

This article not subject to U.S. Copyright. Published 1989 by the American Chemical Society

temperature dependence of $\Delta H$ and $\Delta S$ for unfolding, this does not account for the observed pressure effects on protein denaturation. Nevertheless, the free energy of macromolecular stabilization is a function of temperature, pressure, pH, ionic strength, and the activities of ligands that bind to the folded and/or unfolded states (Schellman, 1987a).

In the present study, we have used Trp and Tyr chromophores as intrinsic probes to spectrally monitor thermally induced changes in exposure of these residues in glutamine synthetase from *Escherichia coli*. Second-derivative absorption spectroscopy was used to monitor solvent accessibility to Tyr residues without interference from Trp by using a technique developed by Ragone et al. (1984). Simultaneously, changes in Trp exposure were measured by UV difference spectroscopy. An advantage of this approach is the ability to monitor unfolding reactions independently in the same or different protein domains. Recently, Ragone et al. (1987) have used second-derivative spectroscopy to monitor Tyr exposure in different domains of myoglobin.

Glutamine synthetase from *E. coli* is a very large, dodecameric metalloenzyme with $M_r$ 622 000 (Ginsburg, 1972; Stadtman & Ginsburg, 1974). Nonetheless, the protein is unusually stable at elevated temperatures. A heat step at 65 °C in the presence of 10 mM $MnCl_2$ gives good yields of the enzyme in the purification procedure of Woolfolk et al. (1966). This paper describes reversible thermal transitions of dodecameric glutamine synthetase and some effects of substrates and metal ions on the stabilization of this enzyme. We have attempted to correlate some of these observations with the X-ray crystallographic structure of Almassy et al. (1986).

## Materials and Methods

*Enzyme Solutions.* Unadenylylated glutamine synthetase (GS)[1] preparations contained an average of 0.8 equiv of covalently bound 5′-adenylate groups per dodecamer as determined by assay (Stadtman et al., 1979) and UV spectra (Ginsburg et al., 1970). GS was purified by the procedure of Woolfolk et al. (1966). Final specific activities in the γ-glutamyl transfer assay at pH 7.57 and 37 °C (Stadtman et al., 1979) were 120 units/mg for GS from *E. coli* W used in initial studies and 135 units/mg for GS purified from an overproducing strain of *E. coli* (Maurizi & Ginsburg, 1986) used for the remainder of the studies. Fully adenylylated enzyme ($GS_{12}$) contained an average of 11.8 equiv of covalently bound 5′-adenylate groups per dodecamer and was prepared in vitro by $Mn^{2+}$-supported adenylyltransferase-catalyzed adenylylation of GS. Adenylyltransferase (a gift from S. G. Rhee of this laboratory) was purified by the procedure of Caban and Ginsburg (1976). An adenylylation reaction containing 50 mg of GS, 1 mM ATP, 5 mM $MnCl_2$, and ~5000 units of adenylyltransferase in 10 mL of 25 mM Tris buffer at pH 8.0 was incubated for 60 min at 37 °C and then overnight at 4 °C; adenylylation was complete as determined by assaying at pH 7.57 ($Mn^{2+}$ ± 60 mM $Mg^{2+}$) with the method of Stadtman et al. (1979).[2] $GS_{12}$ was repurified as described before (Ginsburg et al., 1970). All glutamine synthetase preparations were stored at 4 °C as suspensions in 50% $(NH_4)_2SO_4$ containing 5 mM $MnCl_2$ and 5 mM imidazole (pH 7.1); protein was collected as needed by centrifugation and dialyzed at 4 °C for ~36 h against three changes of 1000-fold volumes of buffer, which usually contained 50 mM Hepes/KOH, 100 mM KCl, and 1.0 mM $MnCl_2$ at pH 7.30 (30.0 °C[3]). After dialysis, enzyme solutions were clarified by centrifugation, and protein concentrations were determined from published absorption coefficients (Ginsburg et al., 1970); a subunit $M_r$ = 50 000 was used to calculate the equivalents of active sites or of subunits. Protein dilutions were made with the final dialysate in each case. The divalent cation–free apoenzyme was prepared as described by Hunt and Ginsburg (1980). For the experiments in which the $Mn^{2+}$ concentration was varied, 6 L of buffer containing 50 mM Hepes/KOH and 100 mM KCl, pH 7.3–7.4, was first treated with Chelex (100–200 mesh; Bio-Rad) in the $K^+$ form; a standardized 0.486 M solution of $MnCl_2$ in 10 mM HCl was added to the indicated final concentration, and the pH was adjusted with HCl if necessary to be pH 7.30 ± 0.02 at 30 °C. Glutamine synthetase (~6 mg) in 1 mM $MnCl_2$ then was dialyzed at 4 °C against three to four changes of 1000-fold volumes of buffer at a given $[Mn^{2+}]$ to ensure equilibration at each free concentration of $Mn^{2+}$, and subsequent protein dilutions were made with the final dialysate. This procedure has been used to determine affinity constants for $Mn^{2+}$ binding to GS (4–27 °C) and gives reliable free concentrations of $Mn^{2+}$ (Hunt et al., 1975; Hunt & Ginsburg, 1980). Substrates were prepared in the final protein dialysate buffer before addition to enzyme solutions. The fully inactive transition-state analogue complex with each active site of GS blocked by the binding of L-Met-(*S*)-sulfoximine phosphate, ADP, and 2 $Mn^{2+}$ (Maurizi & Ginsburg, 1982a) was prepared as described by Maurizi and Ginsburg (1986) and dialyzed against three to four changes of 500-fold volumes of 50 mM Hepes/KOH, 100 mM KCl, and 1.0 mM $MnCl_2$, pH 7.30 at 30 °C.

*Chemicals.* L-Met-(*SR*)-sulfoximine, ADP, ATP, L-glutamine, Hepes, and Tris were purchased from Sigma. The preparation of metal ion free L-glutamine, stock solutions of ADP, and standardized $MnCl_2$ was as described by Hunt et al. (1975); the concentration of L-Met-(*SR*)-sulfoximine was determined by a modified ninhydrin analysis (Shrake et al., 1980). Chelex 100 (100–200 mesh) was from Bio-Rad. Other chemicals were reagent grade. All aqueous solutions were made with distilled water that was deionized and filtered through a Millipore Milli Q2 reagent grade system.

*pH Measurements.* A Radiometer pH meter 26 equipped with a Radiometer combined glass electrode type GK 2322C was used after standardization at 30.0 °C with pH 6.865 and pH 4.015 reference buffers (Leeds & Northrup, 103002 and 103001, respectively). Values for $\Delta pH/\Delta T$ of −0.015 for Hepes buffer, −0.0116 for enzyme assay mixtures as given in the legend to Figure 8 below, and −0.0089 pH unit/°C for the same assay mixture without L-glutamine were used to adjust the pH at 30.0 °C to the value required to give pH 7.0 at the assay temperature. In addition, the pH values of small volumes of the assay mixtures (with and without L-glutamine) were measured at the temperature of assay, and if not pH 7.0 ± 0.04, the pH of each stock assay solution was readjusted accordingly at 30.0 °C.

*Enzyme Assays.* Glutamine synthetase activity was assayed by γ-glutamyl transfer (Stadtman et al., 1979). The pH

[1] Abbreviations: GS and $GS_{12}$, glutamine synthetase from *E. coli* containing 0.8 equiv (unadenylylated) and 11.8 equiv (fully adenylylated) of covalently bound 5′-AMP/dodecamer, respectively; L-MetSox, L-Met-(*SR*)-sulfoximine; MSoxP, L-Met-(*S*)-sulfoximine phosphate (L-*S* and L-*R* diastereoisomers of L-methionine *S*-oxide *S*-imide); Hepes, 4-(2-hydroxyethyl)-1-piperazineethanesulfonic acid; Tris-HCl, tris(hydroxymethyl)aminomethane hydrochloride; Gdn·HCl, guanidine hydrochloride.

[2] This procedure results in a stable $GS_{12}$ product without significant reversal of adenylylation during prolonged incubations as is observed with a $Mg^{2+}$-supported adenylyltransferase reaction in the presence of L-glutamine (Caban & Ginsburg, 1976).

[3] All pH values are reported for 30.0 °C; conditions were pH 7.30 ± 0.02 at 30.0 °C unless otherwise stated.

adjustments of assay components were as described above. The reaction was determined to be linear with respect to both time and enzyme concentration at all temperatures. $K_m$ values for L-glutamine at different temperatures were obtained by varying [Gln] with other assay components as given in the legend to Figure 8 by mixing different proportions of two assay mixtures prepared with 0 and 208 mM L-glutamine, pH 7.0 at the temperature of reaction. The same amount of enzyme in 20 μL was added to initiate reactions in preincubated 1.98, 0.98, and 0.48 mL (standard volume) of assay mixtures for the range of 0.5–3.0, 2–20, and 20–205 mM final L-glutamine concentrations, respectively. At 4- and 2-fold reaction volumes, 4- and 2-fold more concentrated $FeCl_3$–trichloroacetic acid solutions (Stadtman et al., 1979), respectively, were used to stop the reactions. Absorbance values were corrected with blanks obtained from incubations without enzyme (with L-glutamine) and without L-glutamine (with enzyme). A double-reciprocal plot of relative velocity ($A_{540}$) vs L-glutamine concentration at each temperature was fit by a linear least-squares program (e.g., see Figure 9), and the $K_m^{Gln}$ value was obtained from the slope and $y$ intercept.

*Measurements of Temperature-Induced UV Difference Spectra.* A Cary Model 15 spectrophotometer with 0–0.1-A slidewire and reference compartment at 25.0 ± 0.2 °C was used in earlier studies. Later, a Perkin-Elmer 320 spectrophotometer with a scale expansion of ±0.01 A on autorange and the reference cell block at 20.0 ± 0.2 °C was used. The sample cell used in both instruments was a water-jacketed silica cell (1 mL) of 1-cm path length (Precision Cells, Inc.), which was masked with black tape. This cell was connected to an identical water-filled cell (out of the light path in the sample compartment) into which a Teflon-coated thermistor probe (Yellow Springs Instrument Co.) was inserted for monitoring the temperature of the sample cell contents by measuring the resistance (1000 Ω at 25.0 °C). The temperature of the sample cell was controlled to ±0.1 °C by circulating water from a constant-temperature bath (Haake). The thermistor probe was calibrated against a standardized thermometer. Temperature difference spectra were recorded with the same protein solutions in the sample and reference cells. At least three scans were averaged after time-dependent changes were complete (5–20 min), and at >50 °C, spectra usually were recorded only from ~300 to 287 nm. After the highest temperature was reached, the sample cell was disconnected from the hot circulating water and either reconnected to a water bath at 25 °C or equilibrated to the 20 °C block temperature of the Perkin-Elmer; cooling was complete within 5 min. Base-line scans in which the sample and reference cells were at the same temperature were made both initially and after cooling from high temperatures for 30–60 min. Absorbance values obtained at each temperature were corrected for base lines. Peak–trough absorbance differences were measured as a function of temperature and were converted to $\Delta\epsilon$ values in units of $(M\ subunit \cdot cm)^{-1}$. Essentially the same results were obtained with the Cary Model 15, the Perkin-Elmer Model 320, and the Hewlett Packard Model 8450A spectrophotometers (by monitoring absorbances at ~295–290 nm) although the greater sensitivity of the last two instruments allowed reliable measurements to be made with 7-fold lower protein concentrations than required in the earlier studies.

*Light-Scattering Measurements.* Changes in 90° light scattering were measured with a Perkin-Elmer 650-40 fluorescence spectrophotometer with both emission and excitation wavelengths set at 300 nm (4-nm slits). Cuvettes were housed in a water-jacketed cell holder. No changes occurred in observed light scattering (10.8 ± 0.2 relative units) for glutamine synthetase at 76 μg/mL in 20 mM Hepes, 100 mM KCl, and 1.0 mM $MnCl_2$, pH 7.3, during heating of the Mn·enzyme from 20 to 53 °C or while kept at 53 °C for 30 min; this indicates that <3% of the total dodecameric enzyme dissociated or aggregated under these conditions. After the addition of a 4-fold molar excess of EDTA to $Mn^{2+}$ in the protein sample at 53 °C, however, the light-scattering value slowly increased from 10.8 to ~20 relative units, thereby indicating that the apoenzyme aggregated to some extent during incubation at 53 °C.

*Measurements of Temperature-Induced Changes in Tyrosyl Residue Exposure.* Alterations in the dielectric microenvironment surrounding Tyr residues have been demonstrated to be dependent on the ratio ($r$) of two peak to trough second-derivative absorbance differences ($a/b$; see Figure 4B below) in proteins containing Tyr and Trp (Ragone at al., 1984). The observed values of $r$ for the Trp model compounds such as *N*-acetyl-L-tryptophanamide show no significant changes with variations in dielectric medium (Ragone et al., 1984) or temperature (30–65 °C) (M. Fisher, unpublished results). All second-derivative spectra were obtained with a rapid-scan, diode array, UV–visible spectrophotometer (Hewlett Packard Model 8450A), and each is the average of 120 spectra. In the second-derivative spectra, the two maxima utilized were centered at 289 and 295 nm, and the two minima utilized were centered at 285 and 291 nm (Figure 4B). The value of $r$ is defined by Ragone et al. (1984) as

$$r = \frac{a}{b} = \frac{A''(289\ nm) - A''(285\ nm)}{A''(295\ nm) - A''(291\ nm)} \quad (1)$$

where $A''(\lambda)$ is the second-derivative absorbance at wavelength $\lambda$.

The degree of Tyr exposure, $\delta$, is obtained from the equation (Ragone et al., 1984):

$$\delta = \frac{r_n - r_a}{r_u - r_a} \quad (2)$$

$r_n$ and $r_u$ are the numerical values of the ratio $a/b$ determined for the native and unfolded (in 6 M Gdn·HCl) conformers of the protein; $r_a$ corresponds to the ratio obtained when the same molar ratio of Tyr to Trp model compounds as in the protein is present in ethylene glycol and represents a complete burial of all aromatic residues of the protein (Ragone et al., 1984). Glutamine synthetase from *E. coli* contains 17 Tyr and 2 Trp residues (Colombo & Villafranca, 1986). The second-derivative peak–trough ratios $r_a$ and $r_u$ were obtained for the molar ratio (17/2) with the second-derivative molar extinction coefficients of Ragone et al. (1984). Thus, for glutamine synthetase, the calculated values were $r_a = -1.34$ and $r_u = 10.04$ for the complete burial and exposure of tyrosine residues, respectively.

The thermal analysis was performed by using a Hewlett Packard Model 8450A spectrophotometer with a dedicated temperature controller (Model 89100A) and an attached peltier junction temperature-controlled cuvette holder (Model 89101A) with a built-in magnetic stirrer and temperature probe. The reference cuvette contained the protein dialysate buffer and was maintained at 30 °C. The instrument was programmed to increase the temperature in 1 °C increments in the denaturation region with 7-min equilibration times between absorption measurements. Independent measurements on similar samples indicated that the thermal transition was complete within the first minute. After equilibration, 120 absorption spectra were collected at 2 spectra/s. The collected

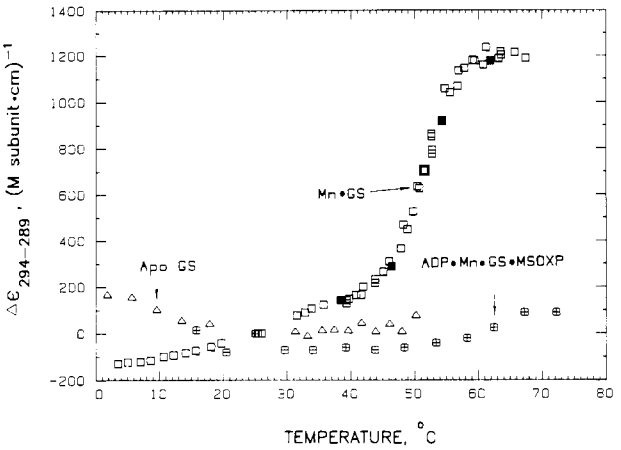


FIGURE 1: Temperature-induced changes in Trp exposure in unadenylylated glutamine synthetase. Peak (~294 nm)–trough (~289 nm) absorbance differences were monitored for unadenylylated glutamine synthetase as a function of temperature by UV difference spectroscopy; the reference cell was thermostated at 25.0 °C. $\Delta\epsilon_{294-289}$ values in (M subunit·cm)$^{-1}$ are plotted as a function of temperature in degrees centigrade. Each protein sample was ~2.3 mg/mL in 50 mM Hepes/KOH and 100 mM KCl, pH 7.3, with or without 1.0 mM $MnCl_2$ present. Data obtained on heating the Mn·enzyme complex (Mn·GS) from 4 to 67 °C (open squares) and on cooling Mn·GS from 67 to 25 °C (closed squares) are shown. The open triangles show $\Delta\epsilon$ values obtained during heating the divalent cation free enzyme (Apo GS) from 2 to 50 °C. The transition-state analogue complex ADP·Mn·GS·MSOXP had L-Met-(*S*)-sulfoximine phosphate, ADP, and 2 $Mn^{2+}$ bound per active site, and data obtained on heating this inactive complex from 16 to 72 °C (crossed ovals) are plotted.

absorption and second-derivative spectra were then averaged. After the thermal transition was complete (i.e., no change in the second-derivative value *r* with further increase in temperature), the protein solution was cooled to the original starting temperature (30 °C) and equilibrated for 15 min; then an absorption spectrum was measured to confirm reversibility. In all cases, the second-derivative spectra obtained on cooling showed no hyteresis in the *r* values, and at 30 °C, the measured spectra yielded the original *r* value.

## Results

Glutamine synthetase undergoes a reversible, thermally induced transition as monitored by changes in Trp exposure. These data are compatible with a two-state model for partial unfolding. Changes in Tyr exposure are also compatible with a two-state model for partial unfolding, which gives different parameters from those for the Trp data, thereby suggesting independent transitions (random model). Transition temperatures ($T_m$ values) for these transitions are a strong function of $Mn^{2+}$ concentration. Responses of the two $T_m$ values to changes in $Mn^{2+}$ concentration are closely parallel, thereby suggesting linked transitions. The data also are shown to be in accord with a sequential model. Steady-state kinetic parameters were measured throughout the temperature range of the transitions in order to detect any manifestation of these in the catalytic properties of the enzyme.

*Temperature-Induced Changes in Tryptophanyl Residue Exposure.* On heating glutamine synthetase in buffer containing 1 mM $MnCl_2$ and 100 mM KCl, pH 7.3,[3] a difference spectrum developed corresponding to perturbation of Trp and Tyr chromophores (Figure 4A below). A plot of the peak–trough differences (centered at ~294 and ~289 nm, respectively) corresponding to the Trp perturbation shows a sigmoidal curve at ≥40 °C (Figure 1, squares), indicative of a thermally induced transition taking place in the enzyme. The linear temperature dependence of $\Delta\epsilon_{294-289}$ values below 40 °C, i.e., in the pretransition region, has been shown by Leach and Smith (1972) to relate to exposed hydrated Trp and Tyr residues. At ≥58 °C, an upper limit is reached with a maximum $\Delta\epsilon_{294-289}$ value of ~1100 (M subunit·cm)$^{-1}$ with respect to an extrapolated pretransition base line. This corresponds to the exposure of ~0.7 Trp/subunit if an $\Delta\epsilon_{294-289}$ value of ~1600 (M subunit·cm)$^{-1}$ for the exposure of one Trp (Shrake & Rupley, 1980) is assumed. The thermal transition monitored by the increase in Trp exposure is fully reversible since the same sigmoidal curve was obtained on heating (Figure 1, open squares) and cooling (Figure 1, closed squares); reheating the sample generated an identical transition curve (data not shown). In addition, after heating and subsequent cooling, glutamine synthetase had full enzymatic activity. Separate experiments were conducted to measure light-scattering changes with increasing temperature in order to detect concomitant changes in the aggregation state of this dodecameric protein (see Materials and Methods). No changes in light scattering were detected on heating the Mn·enzyme in 1 mM $MnCl_2$, pH 7.3, from 20 to 53 °C, thereby demonstrating that no dissociation or aggregation of dodecamer takes place in the temperature range of the observed spectral transition.

Increasing the temperature of the catalytically inactive apoenzyme to ~50 °C produced no increase in Trp exposure (Figure 1, triangles). Heating beyond 50 °C caused the apoenzyme to aggregate, but the divalent cation free dodecamer has been shown to be an unstable form (Shapiro & Ginsburg, 1968). The divalent metal ion free enzyme already has approximately one Trp exposed relative to Mn·enzyme since $\Delta\epsilon^{max}_{295-290} = -1560$ (M subunit·cm)$^{-1}$ for binding $Mn^{2+}$ to apoenzyme, but treatment of the apoenzyme with 6 M Gdn·HCl exposes additional Trp (Hunt & Ginsburg, 1972). Apparently, the apoenzyme is in a more open conformation throughout the temperature range studied, and additional Trp exposure is not induced by heating.

The observations with apoenzyme indicate that the native Mn·enzyme complex contains >1 Trp buried per subunit. The thermally induced unfolding of Mn·enzyme, which increases Trp exposure by ~0.7 residue/subunit, therefore does not fully expose Trp. Thus, the high-temperature form of this species is only partially unfolded. Since glutamine synthetase contains 2 Trp/subunit, this partial unfolding involves an increase in Trp exposure that represents a substantial percentage of the total Trp present.

When each active site of the enzyme is occupied by the transition-state analogue L-Met-(*S*)-sulfoximine phosphate, ADP, and 2 $Mn^{2+}$, Trp residues become more buried (Maurizi & Ginsburg, 1982a,b). However, no change in Trp exposure occurred on heating this complex (Figure 1, crossed ovals). The transition-state analogue complex is extremely stable at neutral pH (Maurizi & Ginsburg, 1982b), and these high-affinity, active-site ligands probably remained bound to the enzyme throughout the 16–72 °C temperature range of the experiment in Figure 1. A thermally induced exposure of Trp residues in this complex therefore must occur at >72 °C.

The thermally induced unfolding of native glutamine synthetase (F) to partially unfolded protein (U) at a total molar protein concentration of $E_0$ was analyzed with a two-state model. The equilibrium constant for the process at temperature *T* is defined in terms of experimental parameters in the following way:

$$K_{eq} = \frac{[U]}{[F]} = \frac{[U]}{E_0 - [U]} = \frac{\Delta\epsilon}{\Delta\epsilon_{max} - \Delta\epsilon} \qquad (3)$$

where $\Delta\epsilon$ and $\Delta\epsilon_{max}$ are the change in absorbance at tem-

Table I: Parameters from a Two-State Fit of Thermally Induced 294–289-nm Absorbance Differences (Trp Exposure) for Glutamine Synthetase in the Presence of Various Active-Site Ligands

| enzyme complex[a] | $T_m$ (°C) | $\Delta H_{vH}$ (kcal/mol) | $\Delta\epsilon_{max}$ (M subunit)$^{-1}$ | no. of data points | $\alpha'$[b] |
|---|---|---|---|---|---|
| Mn·GS | 51.1 | 84 | 960 | 35 | 0.99 |
| Mn·GS (2.33 mg/mL) | 50.4 | 76 | 1140 | 11 | 0.96 |
| Mn·GS (0.45 mg/mL) | 49.6 | 95 | 1120 | 12 | 0.92 |
| Mn·GS (pH 7.60)[c] | 49.7 | 95 | 1170 | 11 | 0.94 |
| Mn·GS (pH 6.95) | 47.2 | 76 | 1100 | 7 | 0.98 |
| Mn·$GS_{12}$ (pH 7.1) | 50.9 | 68 | 1270 | 15 | 0.97 |
| Mg·GS (1 mM $MgCl_2$, pH 7.1) | 47.6 | 63 | 1020 | 10 | 0.92 |
| Mg·GS (10 mM $MgCl_2$) | 51.8 | 108 | 950 | 14 | 0.95 |
| ADP·Mn·GS (0.15 mM ADP) | 54.7 | 81 | 550 | 11 | 0.98 |
| Mn·GS·MetSox (1.0 mM MetSox) | 57.4 | 149 | 880 | 13 | 0.99 |
| Mn·GS·Gln·$NH_2OH$ (0.4 mM $MnCl_2$, 50 mM Gln, 0.5 mM $NH_2OH$) | 57.3 | 89 | 1070 | 4 | 0.94 |
| Mn·GS·Gln·$NH_2OH$ (0.4 mM $MnCl_2$, 50 mM Gln, 20 mM $NH_2OH$) | 56.6 | 81 | 940 | 7 | 0.89 |
| Mn·GS·Gln (100 mM Gln) | 59.0 | 105 | 810 | 17 | 0.98 |
| Mn·GS·Gln (150 mM Gln) | 59.9 | 94 | 810 | 14 | 0.91 |
| ADP·Mn·GS·Gln (0.15 mM ADP, 150 mM Gln) | 68.7 | 99 | 575 | 9 | 0.88 |
| ADP·Mn·GS·MetSox-P | >72 | | | | |

[a] Three different unadenylylated glutamine synthetase (GS) preparations containing an average of 0.8 equiv of covalently bound 5′-AMP per dodecamer and a fully adenylylated enzyme ($GS_{12}$) prepared in vitro (see Materials and Methods) were used. The enzyme (≤2.3 mg/mL) ± ligands was in 20 or 50 mM Hepes/KOH, 100 mM KCl, and 1.0 mM $MnCl_2$ adjusted to pH 7.30 ± 0.02 at 30 °C unless otherwise indicated. [b] This is the greatest value of $\alpha$ ($\alpha = \Delta\epsilon/\Delta\epsilon_{max}$) obtained experimentally. [c] All pH values are given for 30 °C measurements.

perature $T$ and the maximum change in absorbance (both with respect to the extrapolated pretransition base line), respectively, and both are in units of (M subunit·cm)$^{-1}$. Figure 2 illustrates a two-state analysis of temperature-induced partial unfolding for glutamine synthetase in the presence of the active-site ligands $Mn^{2+}$ (1.0 mM) and L-Met-(*SR*)-sulfoximine (1.0 mM) at pH 7.3. The linear pretransition base line is extrapolated by linear least-squares into the transition region in order to subtract these base-line values from experimental $\Delta\epsilon$ values throughout the transition. Typically the pretransition base line had a slope of 5.0 (M subunit·cm·°C)$^{-1}$ although this value varied somewhat in the presence of different ligands, thereby reflecting different extents of Trp and Tyr chromophore exposure to bulk solvent in the native enzyme complexes (Leach & Smith, 1972). The slope of the posttransition (high temperature) base line may differ from that of the pretransition base line but is difficult to establish experimentally. The posttransition base line therefore is assumed to have the same slope as the pretransition base line.

For a two-state reaction, a van't Hoff temperature dependence of the free energy change ($\Delta G$) gives the expression for the equilibrium constant ($K_{eq}$) at temperature $T$ in degrees kelvin:

$$K_{eq} = \exp\left\{\frac{-\Delta H_{vH}}{R}\left(\frac{1}{T} - \frac{1}{T_m}\right)\right\} \quad (4)$$

where $\Delta H_{vH}$ is the temperature-independent van't Hoff enthalpy of reaction in kilocalories per mole of reacting unit, $T_m$ is the transition temperature in degrees kelvin ($\Delta G_{unfolding} = 0$ at $T_m$), and $R$ is the gas constant in kilocalories per mole per degrees kelvin.[4] Thus, calculated values of $\Delta\epsilon$ at temperature $T$ ($\Delta\epsilon^{calcd}$) may be computed with values of $T_m$, $\Delta H_{vH}$, and $\Delta\epsilon_{max}$ by rearranging eq 3 to give

$$\Delta\epsilon^{calcd} = \frac{\Delta\epsilon_{max} K_{eq}}{1 + K_{eq}} \quad (5)$$

For an unfolding experiment, all experimental $\Delta\epsilon$ values (after subtracting the extrapolated low-temperature base line) were simultaneously fit with corresponding $\Delta\epsilon^{calcd}$ values by adjustment of the parameters $T_m$, $\Delta H_{vH}$, and $\Delta\epsilon_{max}$ with a nonlinear least-squares program to minimize the sum of the squares of the differences between the experimental $\Delta\epsilon$ and the $\Delta\epsilon^{calcd}$ values, i.e., the residuals. The best-fit parameters obtained for the partial unfolding of Mn·enzyme in the presence of 1.0 mM L-Met-(*SR*)-sulfoximine are given in Table I. A plot of the resultant $\Delta\epsilon^{calcd}$ function over the pretransition base line (Figure 2, solid curve) demonstrates the excellent fit of the calculated curve for the two-state unfolding model to the experimental data. Assuming that the post- and pretransition base lines are parallel may introduce

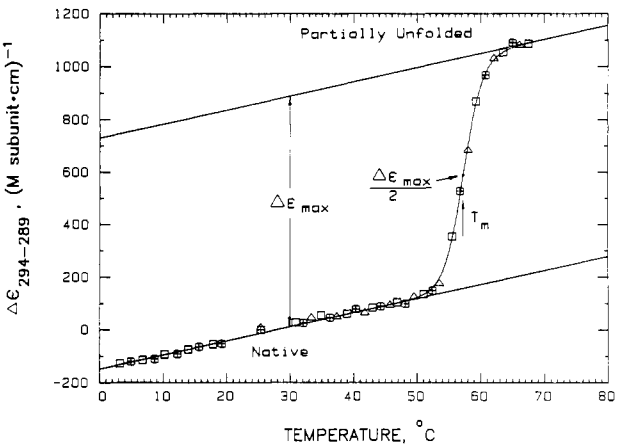


FIGURE 2: Two-state analysis of the thermally induced transition of unadenylylated glutamine synthetase in the presence of L-Met-(*SR*)-sulfoximine as monitored by changes in Trp exposure. $\Delta\epsilon_{294-289}$ values were measured and plotted as in Figure 1. Each sample consisted of ~2.3 mg/mL unadenylylated glutamine synthetase in 50 mM Hepes/KOH, 100 mM KCl, and 1.0 mM $Mn^{2+}$, pH 7.3, with 1.0 mM L-Met-(*SR*)-sulfoximine. Data from three different heating experiments with different samples (squares, crossed ovals, and triangles) are plotted over the range 3–68 °C. The predenaturation base line obtained by linear least-squares fitting of data from 3 to 48 °C is extrapolated to 80 °C (lower solid line). After subtraction of the pretransition base line, $\Delta\epsilon$ data in the thermal transition region (49–67 °C) were fit by nonlinear least squares by simultaneously adjusting $T_m$, $\Delta H_{vH}$, and $\Delta\epsilon_{max}$ (see Results); best-fit values of these parameters (Table I) were used to plot $\Delta\epsilon^{calcd}$ (eq 4 and 5) vs temperature with respect to the pretransition base line (solid curve). The posttransition base line is extrapolated to 0 °C (upper solid line) parallel to the predenaturation line; the calculated value of $T_m$, which occurs at $\Delta\epsilon = \Delta\epsilon_{max}/2$, is indicated.

[4] Units of calories are used in this paper; for conversion to the International System of Units (SI), 1.00 cal = 4.184 J.

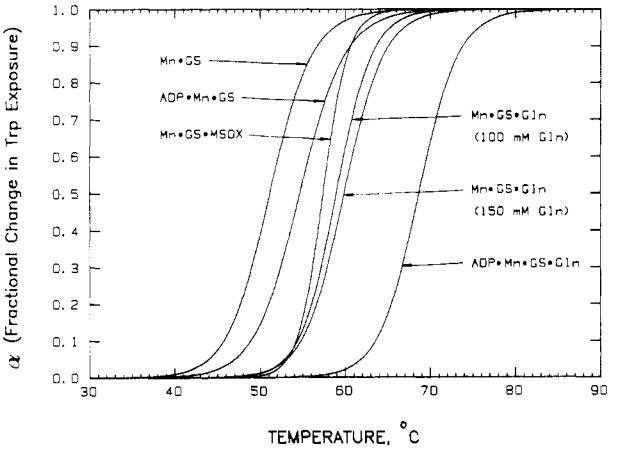


FIGURE 3: Stabilization of unadenylylated glutamine synthetase by substrates. Progress curves are from two-state fits of thermally induced transitions of GS in the absence and presence of substrates as monitored by changes in Trp exposure. Each progress curve is a plot of the fractional change in exposure of Trp, $\alpha$ (where $\alpha = \Delta\epsilon_{294-289}/\Delta\epsilon^{max}_{294-289}$ and all $\Delta\epsilon$ values have the pretransition base line subtracted), vs temperature in degrees centigrade. Enzyme samples were in 50 mM Hepes/KOH, 100 mM KCl, and 1.0 mM $Mn^{2+}$, pH 7.3. For simplicity, the experimental data points are not shown; the corresponding solid curves calculated by using eq 4 and 5 with best-fit values of $T_m$, $\Delta H_{vH}$, and $\Delta\epsilon_{max}$ (Table I) are plotted for the following Mn·enzyme complexes: Mn·enzyme in the absence of added ligands (Mn·GS), Mn·enzyme in the presence of 0.1 mM free ADP (ADP·Mn·GS), Mn·enzyme in the presence of 1.0 mM L-Met-(*SR*)-sulfoximine (Mn·GS·MSOX), Mn·enzyme in the presence of 100 and 150 mM L-glutamine (Mn·GS·Gln), and Mn·enzyme in the presence of 0.1 mM free ADP and 150 mM L-glutamine (ADP·Mn·GS·Gln).

a small error in the thermodynamic parameters, which for comparative purposes is negligible.

Addition of various substrates, ADP, L-Met-(*SR*)-sulfoximine, L-glutamine, and L-glutamine + ADP, to the Mn·enzyme at pH 7.3 was found to stabilize the native form of glutamine synthetase (i.e., to increase $T_m$) to different extents. Plots of progress curves, i.e., $\alpha$ vs $T$ where $\alpha = \Delta\epsilon^{calcd}/\Delta\epsilon_{max}$, computed with the parameters resulting from two-state fits to each set of thermal transition data are given in Figure 3; the corresponding fitted parameters are in Table I. For clarity, experimental data are not shown in Figure 3. In all cases, the data conformed to a two-state model for partial unfolding, as illustrated in Figure 2.

The progress curves in Figure 3 for the partial unfolding of Mn·enzyme (1.0 mM $Mn^{2+}$) in the absence and presence of added ligands demonstrate that the Mn·enzyme in the absence of added ligands is the least stable. The ADP·Mn·GS complex shows the shallowest progress curve whereas the Mn·GS·L-Met-(*SR*)-sulfoximine (Mn·GS·MSOX) complex exhibits the steepest progress curve. The affinity of the Mn·enzyme at pH 7.1 and 30.0 °C increases monotonically for the following ligands: L-glutamine [$K_A' = 140\ M^{-1}$ (Shrake et al., 1977)], L-Met-(*SR*)-sulfoximine [$K_A' = 8300\ M^{-1}$ (Shrake et al., 1982; Gorman & Ginsburg, 1982)], ADP [$K_A' = 3.5 \times 10^5\ M^{-1}$ (Hunt et al., 1975)], and ADP + L-glutamine [$K_A' = 1.7 \times 10^8\ M^{-1}$ (Shrake et al., 1977)]. However, at the ligand concentrations indicated in Figure 3, the free energy of ligand binding to native Mn·enzyme monotonically becomes more negative at 30 °C (and also at a temperature in the middenaturation region) with the following ligands: L-Met-(*SR*)-sulfoximine, L-glutamine, ADP, and ADP + L-glutamine. These relative free energies of binding correlate with the relative values of the corresponding $T_m$ values except for ADP (Table I), which is the poorest thermal stabilizer of native Mn·enzyme of all these ligands. This suggests that ADP also binds to partially unfolded Mn·enzyme. In addition, the $\Delta\epsilon_{max}$ values obtained with ADP are substantially less than those obtained in the absence of ADP. This is compatible with ADP binding to both native and partially unfolded Mn·enzyme so as to decrease Trp exposure to a greater extent in the high-temperature form. The 1 °C higher value of $T_m$ for glutamine synthetase in the presence of the higher L-glutamine concentration (Table I) reflects a more negative free energy of binding to native enzyme.

All thermal transition data measured by an increase in Trp exposure were fit with the two-state model for partial unfolding of glutamine synthetase and reached ≥88% of completion (Table I). Excellent agreement between the fitted and experimental progress curves was found in each case; changes in the best-fit values of the adjustable parameters that are of the order of the estimated errors (see below) cause substantial increases in the sum of the squares of the residuals. The first and second entries in Table I were obtained with different unadenylylated glutamine synthetase preparations in 1.0 mM $Mn^{2+}$ at 2.3 mg/mL and pH 7.3; the reproducibility in the individual $T_m$, $\Delta H_{vH}$, and $\Delta\epsilon_{max}$ values is estimated as ±0.5 °C, ±10 kcal/mol, and ±100 (M subunit·cm)$^{-1}$, respectively. The fact that these parameters at 2.33 and 0.45 mg/ml Mn·enzyme (a 5-fold concentration difference) are the same within experimental error indicates that no change in oligomeric structure occurs during the transition, in accord with the light-scattering results. The fully adenylylated Mn·enzyme may be more thermally stable since $T_m$ at pH 7.1 was approximately the same as that observed at pH 7.3 with the unadenylylated Mn·enzyme, which has a lowered $T_m$ at pH 6.95 (Table I).

The apparent affinity of the native enzyme for $Mn^{2+}$ (and $Mg^{2+}$) is pH dependent (Denton & Ginsburg, 1969; Hunt & Ginsburg, 1972) and decreases substantially with decreasing pH; this is reflected in $T_m$ values for Mn·enzyme (Table I). All experiments were carried out in Hepes buffer ($\Delta pH/\Delta T = -0.015$ pH unit/°C), so that a buffer of pH 7.30 at 30.0 °C has pH 7.00 at 50.0 °C. The slight variation in buffer pH at the $T_m$ of the various protein complexes has no significant effect on the results reported here.

The affinity of unadenylylated glutamine synthetase for $Mg^{2+}$ is less than that for $Mn^{2+}$ at $n_1$ sites (Hunt & Ginsburg, 1972), but the $T_m$ for the enzyme in the presence of either 1.0 mM $Mn^{2+}$ or 10 mM $Mg^{2+}$ is the same within experimental error (Table I), ~51 °C. Thus, the difference in the free energy of divalent metal ion binding to native and partially unfolded enzyme at all sites (net free energy of binding) is about the same with 1.0 mM $Mn^{2+}$ as with 10 mM $Mg^{2+}$.

The active-site ligand L-Met-(*S*)-sulfoximine phosphate when bound to the enzyme has a structure closely analogous to that formed during the course of L-glutamine synthesis (Meister, 1974; Gass & Meister, 1970). The $T_m$ found in the presence of L-Met-(*SR*)-sulfoximine (1.0 mM), 57 °C, is the same within experimental error as that found for the Mn·GS·Gln·$NH_2OH$ complex but 11 °C less than that for the ADP·Mn·GS·Gln complex (Table I). However, a 40-fold reduction in hydroxylamine concentration did not significantly change $T_m$ (Table I); this suggests an interaction of hydroxylamine with both the native and partially unfolded species.

The relative $\Delta H_{vH}$ values presented in Table I are difficult to interpret. The largest $\Delta H_{vH}$ value for the thermally induced unfolding of glutamine synthetase (149 kcal/mol) was observed with the Mn·enzyme in the presence of 1.0 mM L-Met-(*SR*)-sulfoximine. However, $\Delta H_{vH}$ values of ~90 ± 10

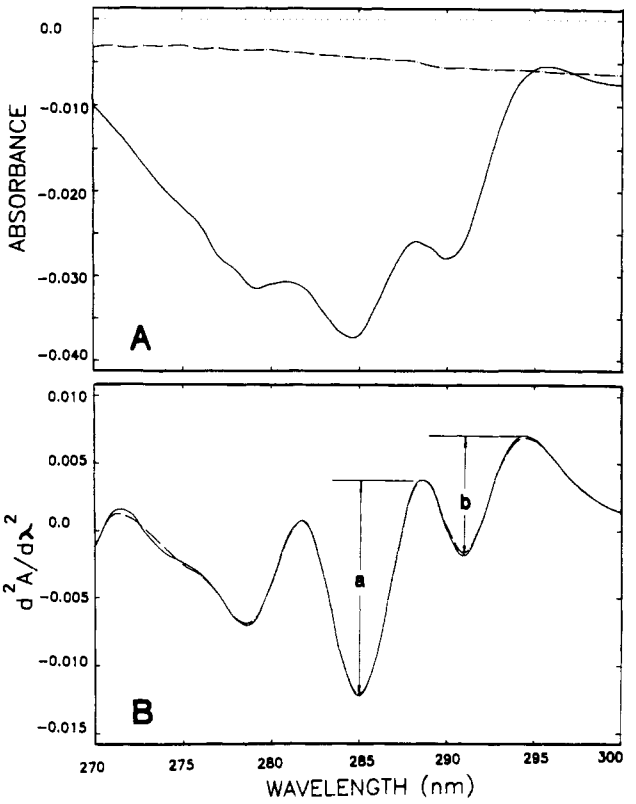


FIGURE 4: Temperature-induced UV difference (A) and second-derivative absorption (B) spectra illustrating the reversible nature of the observed thermal transition centered in the UV region are illustrated for the $Mn^{2+}$- or $Mg^{2+}$-enzyme complex (~1 mg/mL) in the presence of 1 mM $MnCl_2$ or 10 mM $MgCl_2$, 50 mM Hepes, and 100 mM KCl, pH 7.3. Spectra were obtained with a Hewlett Packard 8450A rapid-scan spectrophotometer, and each is the average of 120 scans. In (A), the solid line is the difference spectrum obtained at 57 vs 30 °C, and the dotted and dashed lines are base lines (30 vs 30 °C) before and after heating to 57 °C, respectively. In (B) are shown the initial second-derivative spectrum at 30 °C (solid curve) and the spectrum at 30 °C after heating to 60 °C (dashed line). The enzyme activity remained unchanged after heating and cooling. The two peak–trough differences used to calculate the $r$ value (eq 1, Materials and Methods) are indicated on the second-derivative spectra in (B) as $a$ and $b$.

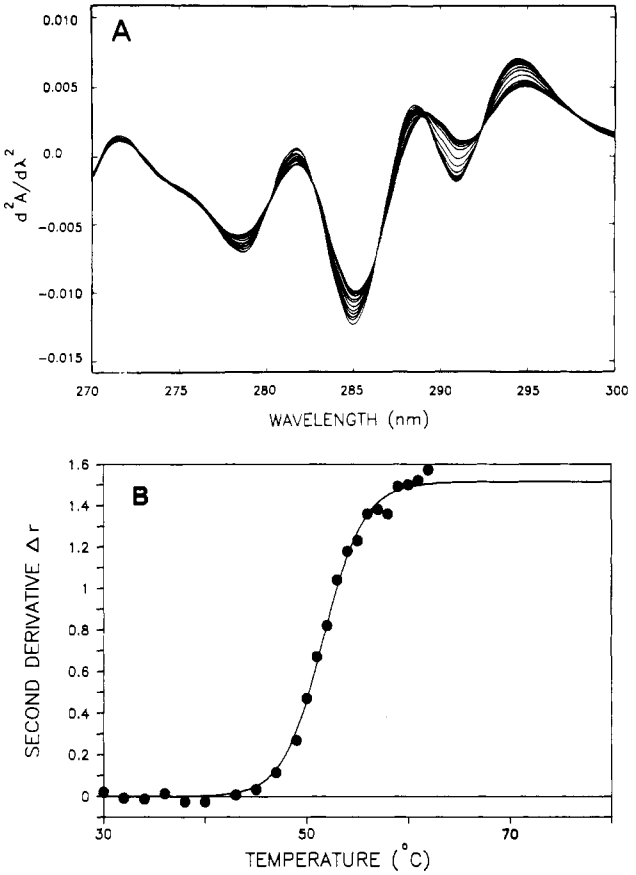


FIGURE 5: Thermally induced second-derivative absorption spectra. The top panel (A) illustrates thermally induced second-derivative spectra for the Mn·GS or Mg·GS complex of Figure 4. As the temperature was increased from 45 to 57 °C, the labeled peak–trough values, $a$ and $b$, in Figure 4B decreased. In (B), corresponding $\Delta r$ values ($r$ – 1.78; see Results) are plotted as a function of temperature (●); these data were fit by assuming an independent two-state unfolding process (see Results). The calculated enthalpy change ($\Delta H_{vH}$) and transition temperature ($T_m$) were 105 kcal/mol and 51.6 °C for Mn·GS (1.0 mM $Mn^{2+}$) for the plot in (B).

kcal/mol were obtained with most of the enzyme complexes; the corresponding average change in entropy for the unfolding reaction, monitored by increase in Trp exposure, is ~280 cal/(mol·K).

*Temperature-Induced Changes in Tyrosyl Residue Exposure.* Temperature-induced difference spectra for glutamine synthetase in buffer containing 1.0 mM $MnCl_2$ or 10 mM $MgCl_2$, at pH 7.3, show Tyr and Trp perturbations. The difference spectrum obtained at 57 vs 30 °C as well as the base line before and after heating to 60 °C (30 vs 30 °C) is shown in Figure 4A; the base lines are essentially parallel. A plot of peak–trough differences at ~288–285 nm vs temperature shows no Tyr perturbation but rather gives a linear temperature dependence of solvent-exposed aromatic chromophores throughout the range 30–61 °C (data not shown). Demchenko (1986) has demonstrated that 289–285-nm absorbance differences commonly used to detect Tyr perturbations are sometimes masked in temperature-induced difference spectra due to interference by Trp perturbations. However, a plot of peak–trough differences at ~281–285 nm (corresponding to a predominant perturbation of Tyr) vs temperature shows a thermal transition (data not presented), but the corresponding $\Delta\epsilon_{max}$ value is less than 400 (M subunit·cm)$^{-1}$. Reliable $T_m$ and $\Delta H_{vH}$ values for the Tyr perturbation therefore are not readily obtained from difference spectra.

Treatment of second-derivative absorption spectra by the method of Ragone et al. (1984) gives extremely reproducible values for absolute Tyr exposure with no interference from Trp perturbations (see Materials and Methods). The second-derivative spectrum for Mn·enzyme at 30 °C obtained before heating is presented in Figure 4B (solid line), and that at 30 °C obtained after heating to 60 °C is also presented in Figure 4B (dashed line); lines $a$ and $b$ indicate the peak–trough differences used to compute the $r$ values (eq 1; Materials and Methods). The coincidence of the two second-derivative spectra in Figure 4B demonstrates reversibility. For the $Mn^{2+}$- or $Mg^{2+}$-enzyme at 30 °C, $r$ = 1.78, which corresponds to exposure to solvent of 4.7 (27%) of the 17 Tyr/subunit. The same $r$ value was observed at 30 °C also for all enzyme complexes that had $n_1$ sites occupied by $Mn^{2+}$, i.e., at $Mn^{2+}$ concentrations ≥10 μM.

The second-derivative absorption spectra of Mn·enzyme exhibit a temperature-dependent perturbation; these spectra were measured at 13 temperatures over the range 45–57 °C and are plotted in Figure 5A. Seven local extrema and isosbestic points are present from 270 to 300 nm. The presence of the isosbestic points is indicative of a thermally induced two-state process. Values of $r$ (eq 1; Materials and Methods) were calculated for each of the second-derivative spectra in Figure 5A, and the differences relative to the pretransition base line ($\Delta r$ values) are plotted in Figure 5B (●) as a function of

Table II: Random and Sequential Two-State Analysis of Temperature-Induced Spectral Perturbations of Glutamine Synthetase with Varying $Mn^{2+}$ Concentrations[a]

| free concn of $Mn^{2+}$ at 4 °C (M × $10^6$) | from absorbance differences, 295–290 nm: Trp exposure[b] | | | from second-derivative peak–troughs: Tyr exposure[c] | | | |
|---|---|---|---|---|---|---|---|
| | $T_m$ (°C) | $\Delta H_{vH}$ (kcal/mol) | $\Delta\epsilon_{max}$ (M subunit)$^{-1}$ | $T_m$ (°C) | $\Delta H_{vH}$ (kcal/mol) | $\Delta r_{max}$ | max ΔTyr exposed[e] (M subunit)$^{-1}$ |
| 3.55 | 45.9 (47.8) | 69 (50) | 840 (790) | 48.6 (46.8) | 90 (67) | 1.39 (1.44) | 2.0 (2.0) |
| 10.0 | 49.3 (50.1) | 61 (44) | 823 (902) | 51.8 (50.2) | 85 (65) | 1.22 (1.24) | 1.7 (1.8) |
| 33.0 | 52.3 | 67 | 890 | nd[d] | | | |
| 48.6 | 52.6 (56.2) | 79 (52) | 815 (803) | 55.7 (52.0) | 72 (39) | 1.14 (1.21) | 1.4 (1.5) |
| 292 | 52.1 (54.2) | 87 (63) | 980 (1060) | 54.4 (52.0) | 90 (53) | 1.32 (1.24) | 2.0 (1.8) |
| 1000 | 50.0 (51.3) | 92 (73) | 1060 (851) | 51.6 (49.7) | 105 (67) | 1.51 (1.56) | 2.3 (2.4) |
| 3000 | 46.3 (48.0) | 85 (65) | 1100 (1080) | 48.6 (47.0) | 109 (76) | 1.61 (1.65) | 2.4 (2.5) |
| 5000 | 45.0 | 88 | 1200 | nd[d] | | | |
| 10000 | 41.7 (43.2) | 96 (72) | 1150 (1130) | 43.6 (41.8) | 106 (66) | 2.00 (2.07) | 3.0 (3.1) |

[a] Samples of unadenylylated glutamine synthetase (~6 mg of GS) were dialyzed at 4 °C against three to four changes of 1000-fold volumes of the indicated concentration of $MnCl_2$ in 50 mM Hepes/KOH and 100 mM KCl buffer at pH 7.3 ± 0.02 (at 30 °C) and then diluted to a protein concentration of 0.46–1.0 mg/mL (9–20 μM subunit) with the final dialysate for spectral studies. [b] Nonparenthetical values result from the random model (independent transitions); best-fit values from simultaneous three-parameter, iterative, nonlinear fits (eq 4 and 5) of data (Δε vs $T$), obtained with different spectrophotometers and enzyme samples, were averaged (see Figure 6 for the variation in $T_m$ values). The experimentally measured Δε was ≤0.95 $\Delta\epsilon_{max}$ in all cases. Parenthetical values result from the sequential model; best-fit values of simultaneous six-parameter, iterative, nonlinear fits (eq 7a,b) of data (Δε vs $T$ and Δ$r$ vs $T$) are presented. [c] Nonparenthetical values result from the random model; see Figure 5B, eq 1, 4, and 5, and text. Three-parameter fits of second-derivative Δ$r$ vs $T$ data for $T_m$, $\Delta H_{vH}$, and $\Delta r_{max}$ values were made. Parenthetical values are as in footnote *b*. [d] Not determined. [e] Maximum ΔTyr exposed were determined by using eq 2 to determine the percentage of Tyr residues exposed for low-temperature ($r$ = 1.78) and high-temperature ($r$ = 3.0–3.8) conformers. For calculating the maximum ΔTyr exposed, 17 Tyr/subunit is used.

temperature and show sigmoidal behavior, indicating a temperature-induced increase in Tyr exposure with a $\Delta r_{max}$ value of 1.51 (Table II). The Δ$r$ values are independent of temperature in both the pretransition and posttransition regions.

The experimental Δ$r$ values were fit with a two-state model in the same manner as the Δε values from the Trp perturbation by substituting Δ$r$ and $\Delta r_{max}$ for Δε and $\Delta\epsilon_{max}$, respectively, in eq 5. The resultant values of $T_m$, $\Delta H_{vH}$, and $\Delta r_{max}$ (Table II) give a calculated curve (Figure 5B, solid line) that is in good agreement with experimental data (Figure 5B, ●). A similar fitting procedure for Tyr exposure during heating of the Mg·enzyme complex at 10 mM $MgCl_2$ yielded $\Delta H_{vH}$ = 124 kcal/mol, $T_m$ = 53.4 °C, and $\Delta r_{max}$ = 1.30 (data not shown). Thus, for Mn·enzyme (1.0 mM $Mn^{2+}$) and for Mg·enzyme (10 mM $Mg^{2+}$), Tyr exposure increases on heating from 4.66 Tyr/subunit to a maximum exposure of ~6.7 Tyr/subunit. This further indicates that the thermally induced unfolding of either the $Mn^{2+}$– or the $Mg^{2+}$–enzyme complex is only partial although a significant portion of the total Tyr is involved, the equivalent of 2 of 17 residues/subunit.

The apoenzyme has an $r$ value of 4.6, indicating an exposure to solvent of an average of 8.9 Tyr/subunit. Thus, more Tyr residues are exposed to solvent in the apoenzyme than in the partially unfolded (high-temperature) form of $Mn^{2+}$– or $Mg^{2+}$–enzyme.

The estimated errors in the individual $T_m$, $\Delta H_{vH}$, and change in Tyr exposure on unfolding values in Table II are ±0.5 °C, ±10 kcal/mol, and ±0.2 Tyr/subunit, respectively. Even though at least 2 Tyr/subunit are perturbed during heating, each calculated progress curve for a two-state unfolding process agrees well with corresponding experimental data; the resulting best-fit values of the adjustable parameters show the same sensitivity to change as those determined from increase in Trp exposure.

*Effect of $Mn^{2+}$ Concentration on the Thermal Stability of Glutamine Synthetase.* The effects of increasing $Mn^{2+}$ concentration on temperature-induced UV spectral changes were explored for several reasons. (1) The apoenzyme could be the high-temperature form (partially unfolded form) of the enzyme with $T_m$ < 2 °C; this suggests that the temperature-induced unfolding of the Mn·enzyme may cause complete release of divalent cations. (2) However, the addition of ADP to

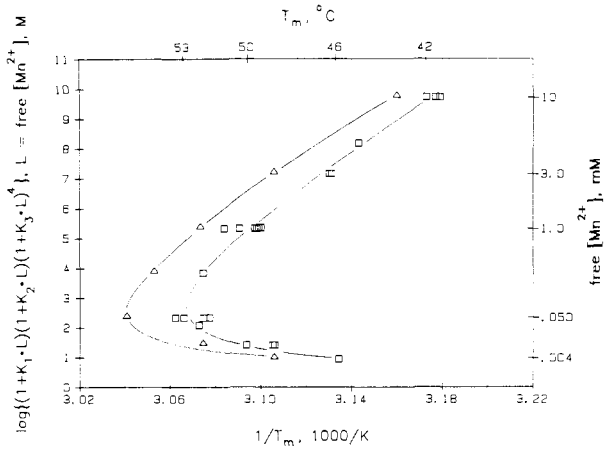


FIGURE 6: Effects of free $Mn^{2+}$ concentration on the thermal stabilization ($T_m$) of unadenylylated glutamine synthetase. The free energy for $Mn^{2+}$ binding to *native* unadenylylated glutamine synthetase is proportional to log $\{(1 + K_1^N L)(1 + K_2^N L)(1 + K_3^N L)^4\}$; this is plotted vs $1/T_m$ with $T_m$ in degrees kelvin, where $K_1^N$, $K_2^N$, and $K_3^N$ are $Mn^{2+}$ binding constants for the $n_1$, $n_2$, and four low-affinity sites in units of (M subunit)$^{-1}$ and $L$ is the *free* $Mn^{2+}$ concentration in molar (see Results and eq 6). $T_m$ values determined from two-state analysis of changes in Trp exposure (□) and Tyr exposure (△) were obtained with the same enzyme samples (0.3–1.0 mg/mL) after exhaustive dialysis at 4 °C against 50 mM Hepes/KOH, 100 mM KCl, and the indicated $Mn^{2+}$ concentration, pH 7.3 (Table II). $T_m$ values result from application of the random model to Trp and Tyr exposure data. Average $T_m$ values for Tyr exposure (△) and all $T_m$ values measured for Trp exposure (□) are plotted as $1/T_m$. The curves (solid lines) are free-drawn.

Mn·enzyme indicates an interaction of this substrate with both native and partially unfolded glutamine synthetase, in which case the high-temperature species may bind $Mn^{2+}$ since ADP binds to $Mn^{2+}$ at $n_2$ sites (Hunt et al., 1975). (3) Glutamine synthetase has two high-affinity, divalent cation sites ($n_1$ and $n_2$) per subunit that must be occupied for activity expression (Hunt et al., 1975); $Mn^{2+}$ binding to $n_1$ sites promotes a large overall conformational change in the protein to an active enzyme form (Shapiro & Ginsburg, 1968; Ginsburg, 1972) that may correlate with increased thermal stabilization of the native enzyme.

$T_m$ values derived from changes in Trp and Tyr exposure as a function of $Mn^{2+}$ concentration were obtained with the

same enzyme samples and are presented in Table II and Figure 6. Trp exposure determined from difference spectra monitored in the Perkin-Elmer Model 320 or Hewlett Packard Model 8450A spectrophotometer was essentially the same. A two-state fit of each data set gives the $T_m$, $\Delta H_{vH}$, and $\Delta\epsilon_{max}$ or $\Delta r_{max}$ values in Table II after averaging the values from experiments performed at the same free $Mn^{2+}$ concentration. A two-state model for unfolding fit to each data set measured by either technique resulted in a computed progress curve that agrees extremely well with experimental data in every case. However, the $T_m$ values obtained for the Trp and Tyr transitions are different at each free $Mn^{2+}$ concentration. Thus, the treatment of the Trp and Tyr data up to now assumes independent two-state transitions. All $T_m$ values for Trp exposure that were obtained from separate fits of experimental data are plotted in Figure 6 (□) in order to demonstrate reproducibility of this parameter whereas average $T_m$ values for Tyr exposure are plotted (Figure 6, Δ). The lower $\Delta\epsilon_{max}$ values for the 295–290-nm absorbance differences at the low $Mn^{2+}$ concentrations in Table II reflect the greater tendency of glutamine synthetase to aggregate at $Mn^{2+}$ concentrations $<10^{-4}$ M.

Schellman (1975, 1976) has described the effect of ligand binding on the transition temperature for the unfolding of a biopolymer. In the case of native glutamine synthetase at pH 7.2, there are two relatively high-affinity [$K_1^N = 2 \times 10^6$ $M^{-1}$ and $K_2^N = 2 \times 10^4$ $M^{-1}$ (Hunt & Ginsburg, 1972)] and four low-affinity [$K_3^N = 500$ $M^{-1}$ (Denton & Ginsburg, 1969)] $Mn^{2+}$ binding sites per subunit. The change in $T_m$ for glutamine synthetase unfolding as a function of free $Mn^{2+}$ concentration is given by

$$\frac{1}{T_m} = \frac{1}{T_m^0} - \frac{R}{\Delta H_{vH}}\left\{\ln\left[\frac{(1 + K_1^N L)(1 + K_2^N L)(1 + K_3^N L)^4}{(1 + K_1^U L) \ldots (1 + K_t^U L)}\right]\right\} \quad (6)$$

where $T_m^0$ and $T_m$ are transition temperatures for a two-state unfolding process (i.e., where $\Delta G_{unfolding} = 0$) in the absence and presence of ligand ($L$ = free molar $Mn^{2+}$ concentration), respectively, and $K_i^N$ ($i$ = 1, 2, 3) and $K_j^U$ ($j$ = 1, 2, ..., $t$) are the temperature-independent binding constants of native protein and unfolded protein with $t$ sites, respectively. If the enthalpy of partially unfolding glutamine synthetase is independent of temperature and of free $Mn^{2+}$ concentration and if the enthalpy of $Mn^{2+}$ binding is negligible compared to the enthalpy of partially unfolding, $\Delta H_{vH}$ in eq 6 is the enthalpy of partially unfolding the enzyme. For native glutamine synthetase, little heat is associated with the binding of $Mn^{2+}$ to $n_1$ sites (Hunt et al., 1972), and the assumption that $\Delta H = 0$ for binding $Mn^{2+}$ to all sites in the native or unfolded form is a reasonable approximation since such metal ion binding is often entropically driven. Furthermore, the range of $T_m$ values is small (~11 °C), and the apparent increase in $\Delta H_{vH}$ with increasing $Mn^{2+}$ concentration for both the Trp and Tyr perturbations is slight in both cases for the random model with average values of 80 ± 16 and 94 ± 14 kcal/mol, respectively (Table II).

Since the number of $Mn^{2+}$ binding sites and $K_j^U$ values for the partially unfolded enzyme are not known, $Mn^{2+}$ is assumed for the purpose of plotting not to bind to this high-temperature form. Thus, the denominator of the argument of the logarithm in eq 6 is taken as unity. $T_m$ values from Trp and Tyr exposure changes are plotted in Figure 6 in a $\log\{(1 + K_1^N L)(1 + K_2^N L)(1 + K_3^N L)^4\}$ vs $1/T_m$ format according to eq 6. This logarithm term is proportional to the free energy of $Mn^{2+}$ binding to native enzyme. If $Mn^{2+}$ does not bind to partially unfolded enzyme, the plot should consist of a straight line with a negative slope. From 3.55 to 49 μM $Mn^{2+}$ (corresponding to ~88–100% saturation of $n_1$ sites and to ~50% occupancy of $n_2$ sites), fairly linear plots with negative slopes are obtained in Figure 6. This indicates essentially exclusive binding of $Mn^{2+}$ to native enzyme. However, at >49 μM $Mn^{2+}$, the slopes of the plots in Figure 6 become positive and approach linearity. Thus, at higher $Mn^{2+}$ concentrations, binding to the high-temperature form predominates. The behavior of the plots in Figure 6 indicates that the partially unfolded enzyme has weaker $Mn^{2+}$ binding constants but a greater number of these than has the native, folded enzyme. Determining the number of $Mn^{2+}$ binding sites in the high-temperature form from the $T_m$ data at the higher $Mn^{2+}$ concentrations (Schellman, 1976) is not feasible since the approximation $1 + K_j^U L \approx K_j^U L$ is not valid in this range of $Mn^{2+}$ concentration.

Values of $\Delta r_{max}$ appear to increase significantly at >1 mM $Mn^{2+}$ (Table II); this suggests that additional Tyr exposure can be induced by increasing $Mn^{2+}$ interactions with the high-temperature form. In addition, Trp exposure increases slightly at >1 mM $Mn^{2+}$ (Table II).

All $T_m$ values for the thermally induced partial unfolding of the Mn·enzyme calculated from Tyr second-derivative analysis are higher than those determined from corresponding 295–290-nm Trp peak–trough differences by assuming independent two-state transitions (Table II). Nevertheless, the relative thermal stability of glutamine synthetase as reflected in $T_m$ values as a function of free $Mn^{2+}$ concentration is the same whether the change in Trp or Tyr exposure is monitored. In addition, at a given free $Mn^{2+}$ concentration, $\Delta H_{vH}$ measured from changes in Tyr exposure is greater than that from changes in Trp exposure in every case except one (Table II). Thus, $\Delta H_{vH}$ values in addition to $T_m$ values appear greater for changes in Tyr exposure than corresponding values derived from changes in Trp exposure.

*Sequential Model for Transitions Monitored by Tryptophan and Tyrosine Exposure Changes.* The responses to change in the free $Mn^{2+}$ concentration of $T_m$ for the Trp and Tyr transitions, determined by assuming independent two-state processes, are parallel (see Figure 6). All $T_m$ values for the thermally induced partial unfolding of the Mn·enzyme calculated from Tyr second-derivative analysis are consistently 2–3 °C higher than those determined from corresponding 295–290-nm Trp peak–trough differences (Table II). This result suggests that the Trp and Tyr transitions may not occur independently but rather are linked with the Trp transition occurring first upon increasing temperature. For such a model, consisting of two sequential two-state unfolding reactions, the progress curves for the Trp and Tyr transitions are given by eq 7a and 7b, respectively, where subscripts 1 and 2 refer to

$$\Delta\epsilon = \frac{\Delta\epsilon_{max} K_{eq}^{(1)}(1 + K_{eq}^{(2)})}{1 + K_{eq}^{(1)}(1 + K_{eq}^{(2)})} \quad (7a)$$

$$\Delta r = \frac{\Delta r_{max} K_{eq}^{(1)} K_{eq}^{(2)}}{1 + K_{eq}^{(1)}(1 + K_{eq}^{(2)})} \quad (7b)$$

the Trp and Tyr transitions, respectively, and $K_{eq}^{(1)}$ and $K_{eq}^{(2)}$ are as defined by eq 4. Equations 7a and 7b are determined from changes in free energy for the sequential process in which the reference state is the fully folded (native) protein. At each concentration of $Mn^{2+}$, the two experimental progress curves were fit simultaneously by nonlinear least-squares by adjusting

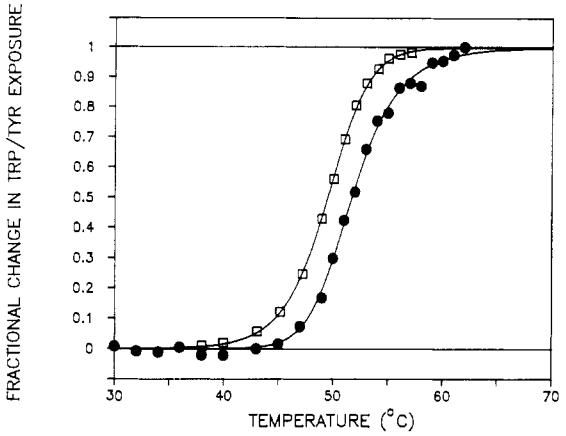


FIGURE 7: Sequential two-state analysis of the thermally induced transitions of unadenylylated glutamine synthetase as monitored by changes in Trp and Tyr exposure. Experimental conditions are as in Figure 6 in 1.0 mM $Mn^{2+}$. $\Delta\epsilon_{294-289}$ values for the change in Trp exposure are normalized with respect to a $\Delta\epsilon_{max}$ value of 851 (M subunit·cm)$^{-1}$ and plotted (□). $\Delta r$ values for the change in Tyr exposure are normalized with respect to a $\Delta r_{max}$ value of 1.56 and plotted (●). $\Delta\epsilon$ and $\Delta r$ data in the transition region were fit to a sequential model by nonlinear least-squares by simultaneously adjusting $\Delta\epsilon_{max}$, $T_m^{(1)}$, $\Delta H_{vH}^{(1)}$, $\Delta r_{max}$, $T_m^{(2)}$, and $\Delta H_{vH}^{(2)}$ (see eq 7a,b and Results); best-fit values of these parameters (Table II) were used to plot the two normalized progress curves.

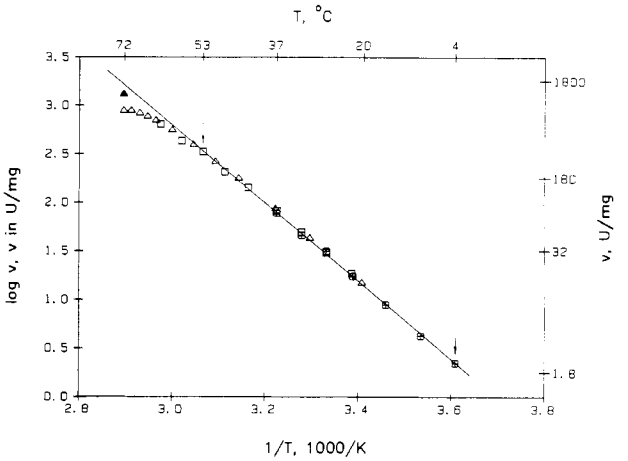


FIGURE 8: Arrhenius plot of γ-glutamyl transfer activity of unadenylylated glutamine synthetase. The γ-glutamyl transfer assay (Stadtman et al., 1979) contained 50 mM Hepes/KOH, 310 mM KCl, 0.4 mM $MnCl_2$, 0.4 mM ADP, 150 mM L-glutamine, 40 mM $NH_2OH$, and 20 mM arsenate, and the pH was adjusted at 30.0 °C in order to maintain pH 7.0 at each temperature. For the end-point assay, both the enzyme concentration and assay time were adjusted to give initial velocities at each temperature. The activities of three different GS samples (crossed ovals, open triangles, and squares) were measured over the range 4–72 °C; velocity, $v$, in units per milligram is plotted as log $v$ vs $1/T$ with $T$ in degrees kelvin, where 1 unit is 1.0 μmol of γ-glutamylhydroxamate formed per minute. Linear least-squares fitting of the data from 4 to 53 °C (denoted by the vertical arrows) gave the solid line, which corresponds to full saturation with substrates and $E_a$ = +18.3 kcal/mol of catalytic site from the slope. The value at 72 °C (open triangle) was corrected to full saturation with L-glutamine and $NH_2OH$ and is shown as the closed triangle.

$\Delta\epsilon_{max}$, $T_m^{(1)}$, $\Delta H_{vH}^{(1)}$, $\Delta r_{max}$, $T_m^{(2)}$, and $\Delta H_{vH}^{(2)}$ to minimize the sum of the squares of the residuals after normalizing each data set to unity in order to weight $\Delta\epsilon$ and $\Delta r$ residuals equally. The best-fit values of these parameters are given in parentheses in Table II. The estimated errors in these parameters are the same as those for values derived from the fit of the random model (independent transitions). At each level of free $Mn^{2+}$, all Tyr data and a representative set of the Trp data were fit. Normalized progress curves are presented in Figure 7 for the sequential model at 1.0 mM free $Mn^{2+}$. These computed progress curves for the changes in Trp and Tyr exposure agree well with corresponding experimental data (Figure 7); changes in the best-fit values of the adjustable parameters that are of the order of the estimated errors cause substantial increases in the sum of the squares of the residuals. Nevertheless, an important conclusion is that the random and sequential models fit the experimental data equally well.

For the random model, the temperatures of half-completion for the two transitions, $T_{0.5}$ values (i.e., where $\Delta\epsilon = \Delta\epsilon_{max}/2$ and $\Delta r = \Delta r_{max}/2$), are identical with the corresponding $T_m$ values in Table II. However, for the sequential model, $T_m^{(1)} > T_{0.5}^{(1)}$ and $T_m^{(2)} < T_{0.5}^{(2)}$, a consequence of the linkage between these sequential two-state transitions; both $T_{0.5}^{(1)}$ and $T_{0.5}^{(2)}$ are complex functions of $T_m^{(1)}$, $\Delta H_{vH}^{(1)}$, $T_m^{(2)}$, and $\Delta H_{vH}^{(1)}$ (eq 7a and 7b). Values of $T_{0.5}$ from the sequential model (data not given) are in reasonable accord with corresponding $T_m$ values from the random model.

For the sequential model, the average $\Delta H_{vH}$ values are 60 ± 11 and 62 ± 12 kcal/mol for the Trp and Tyr transitions, respectively. $T_m^{(1)} \geq T_m^{(2)}$ at all levels of $Mn^{2+}$ (Table II) with differences ranging from 0 to 4 °C. The similar behavior of $T_m^{(1)}$ and $T_m^{(2)}$ is understandable since the obligatory sequential unfolding links the two transitions. Furthermore, as a function of $Mn^{2+}$ concentration, these $T_m$ values show behavior similar to that of $T_m$ values derived from the random model with a maximum in thermal stability of native Mn-enzyme occurring at 49 μM $Mn^{2+}$ (Table II).

*Temperature Dependence of Steady-State Kinetic Parameters.* Glutamine synthetase activity was measured from 4 to 72 °C in order to detect any temperature-induced changes in protein conformation that affect enzymatic activity. For these experiments, the γ-glutamyl transfer reaction

$$\text{L-glutamine} + NH_2OH \xrightarrow[\text{ADP,arsenate}]{Mn^{2+}} \gamma\text{-glutamylhydroxamate} + NH_3 \quad (8)$$

catalyzed by glutamine synthetase (Stadtman & Ginsburg, 1974) was used to study catalytic properties of the unadenylylated Mn-enzyme.

A plot of the logarithm of velocity of $Mn^{2+}$-supported γ-glutamyl transfer activity for the unadenylylated enzyme, $\log(v/E_0)$, vs $1/T$ at pH 7.0 at the temperature of measurement, $T$, is given in Figure 8. If the assay is carried out under saturating conditions, $v = V_{max}$ and such a plot should be linear since

$$V_{max} = E_0 k_{cat} = E_0 \exp\left(\frac{-E_a}{RT}\right) \quad (9)$$

where $V_{max}$ is in units per milliliter, $T$ is in degree kelvin, $E_0$ is the total enzyme concentration, and $E_a$ is the Arrhenius activation energy in kilocalories per mole of catalytic site. The data plotted in Figure 8 are linear from 4 to 53 °C with the slope corresponding to $E_a$ = +18.3 kcal/mol of catalytic site. The deviation from linearity of the plot above 53 °C was found to be due to subsaturating levels of substrates resulting from increased $K_m$ values at the high temperatures rather than to a temperature-induced unfolding of the enzyme. When the measured velocity at 72 °C was corrected to that at saturating levels of L-glutamine ($K_m$ = 17 mM) and hydroxylamine ($K_m$ = 22 mM), this corrected velocity (Figure 8, solid triangle) was increased almost to the extrapolated straight line. Additional correction of log $(v/E_0)$ for slight subsaturation of the enzyme with the nonconsumable substrates ADP and arsenate at >53 °C would make the Arrhenius plot linear over the

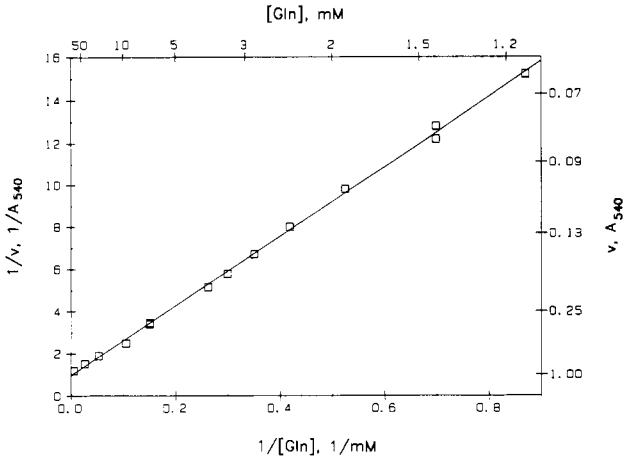


FIGURE 9: Double-reciprocal plot of velocity vs L-glutamine concentration for γ-glutamyl transfer at pH 7.0 catalyzed by unadenylylated glutamine synthetase (2.05–8.20 μg/mL) at 72 °C with 30-s assay times. Assay conditions were as given in the legend to Figure 8 but with varying L-glutamine concentrations. The reciprocal of the relative velocity, $v$, in $A_{540}$ (for γ-glutamylhydroxamate formed) vs $1/[Gln]$ in $mM^{-1}$ is plotted (□). The data were fit by linear least squares (solid line), and $K_m$ is 17 mM as determined from the slope and $y$-axis intercept.

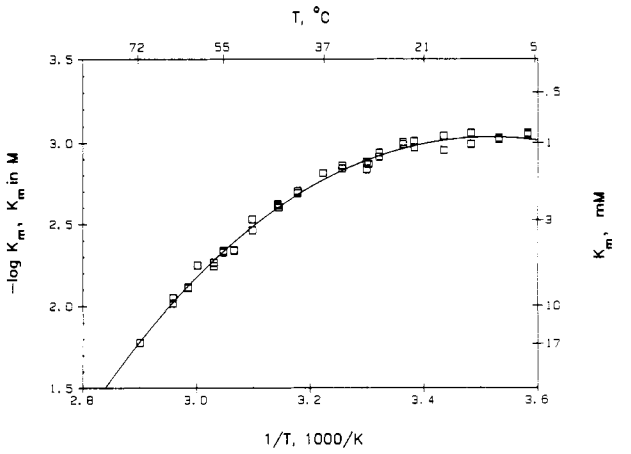


FIGURE 10: van't Hoff plot of $K_m$ for L-glutamine in $Mn^{2+}$-supported γ-glutamyl transfer catalyzed by unadenylylated glutamine synthetase. The $K_m$ values were obtained from double-reciprocal plots of velocity vs L-glutamine concentration as illustrated in Figure 9. Values of $K_m$, plotted as $-\log K_m$ vs $1/T$ (□), were fit by an iterative Simplex procedure (Noggle, 1985) by simultaneously adjusting $\Delta H_{vH}$, $\Delta C_p$, and $K_m^0$ (eq 10). The solid curve was calculated from eq 10 and the best-fit values: $\Delta H_{vH} = -8.58$ kcal/mol, $\Delta C_p = -322$ cal/(mol·K), and $K_m^0$ ($K_m$ at 37.2 °C) = 1.7 mM.

entire temperature range studied.

The temperature dependence of $K_m$ for L-glutamine in γ-glutamyl transfer (reaction 8) also was measured from 5 to 72 °C. Figure 9 is a representative double-reciprocal plot of the observed velocity, $v$, vs L-glutamine concentration at 72 °C, pH 7.0, for which 30-s assays were used. Extremely little scatter in the data in the linear plot of Figure 9 demonstrates the feasibility of measuring $K_m$ values at elevated temperatures with short assays times. The calculated $K_m$ value for L-glutamine was 17 mM at 72 °C.

Previously, the $K_m$ for L-glutamine in reaction 8 with unadenylylated enzyme was found to approximate the $K_D'$ value (Shrake et al., 1977). Assuming $K_m$ for L-glutamine equals $K_D'$ for L-glutamine under conditions of assay permits a van't Hoff analysis of the $K_m$ data from

$$K_m = K_m^0 \exp\left\{\frac{\Delta H^0_{Gln}}{R}\left(\frac{1}{T} - \frac{1}{T_0}\right) + \frac{\Delta C_p}{R}\left[1 - \frac{T_0}{T} - \ln\left(\frac{T}{T_0}\right)\right]\right\} \quad (10)$$

$K_m^0$ is $K_m$ for L-glutamine at the arbitrary reference temperature $T_0$ (37.2 °C) with $T$ and $T_0$ in degree kelvin, $\Delta H^0_{Gln}$ is the temperature-dependent van't Hoff enthalpy of binding L-glutamine under conditions of assay at reference temperature $T_0$ in kilocalories per mole of catalytic sites, and $\Delta C_p$ is the temperature dependence of the enthalpy of L-glutamine binding, $\Delta H_{Gln}$, i.e.

$$\Delta H_{Gln} = \Delta H^0_{Gln} + \Delta C_p(T - T_0) \quad (11)$$

If the change in heat capacity of L-glutamine binding, $\Delta C_p$, is zero, eq 10 predicts that a plot of $-\log K_m$ vs $1/T$ is linear with a slope of $-\Delta H_{Gln}/(2.303R)$; thus, the experimental $K_m$ values for L-glutamine are plotted in this format in Figure 10 (□). The nonlinearity of the plotted data suggests two extreme alternatives: (a) A biphasic plot of two linear segments with a crossing point at ~37 °C arises from two temperature-independent $\Delta H_{Gln}$ values for native and partially unfolded glutamine synthetase forms. With the assumption that $\Delta C_p = 0$, a linear least-squares fit to the data below and above 37.2 °C results in $\Delta H_{Gln}$ values of −3.04 and −14.2 kcal/mol, respectively, corresponding to temperature-independent van't Hoff enthalpies of L-glutamine binding for the low-temperature (native) and high-temperature (partially unfolded) enzyme forms (fitted lines not shown). (b) A single $\Delta H^0_{Gln}$ value with $\Delta C_p \neq 0$ for native glutamine synthetase generates a plot that is concave downward. A nonlinear least-squares fit of all the data assuming a single native enzyme form with $\Delta C_p \neq 0$ gives $\Delta H^0_{Gln} = -8.58$ kcal/mol, $\Delta C_p = -322$ cal/(mol·K), and $K_m^0 = 1.7$ mM; the resulting calculated function is plotted in Figure 10 (solid line) and is an excellent fit of the experimental data.

In view of the 66 °C temperature range of the data, the observation that $k_{cat}$ shows normal Arrhenius temperature dependence over the same temperature interval, and the excellent fit of experimental data with the latter alternative, the most reasonable interpretation is a single temperature-dependent $\Delta H^0_{Gln}$ value for the native enzyme. In addition, the enthalpy for L-glutamine binding in the presence of the other assay components (reaction 8) is in the range of $\Delta H$ values measured calorimetrically at 30 °C: −9.7 and −7.4 kcal/mol for binding L-glutamine to unadenylylated subunit in the absence and presence of saturating ADP at pH 7.1, respectively (Shrake et al., 1977). The $\Delta C_p$ value obtained also is reasonable since a $\Delta C_p$ value of $-160 \pm 100$ cal/(mol·K) has been estimated for binding the active-site ligand L-Met-(*S*)-sulfoximine to the Mn·enzyme complex saturated with the ATP analogue 5′-adenylyl imidodiphosphate at pH 7.1 (Ginsburg et al., 1987). Thus, the temperature dependence of $K_m$ for L-glutamine probably results from the temperature dependence of the enthalpy of binding L-glutamine to native glutamine synthetase under assay conditions and not from a temperature-induced conformational change of the enzyme.

## Discussion

Glutamine synthetase undergoes a reversible, temperature-induced unfolding reaction in the presence of $Mn^{2+}$ or $Mg^{2+}$ as evidenced by perturbation of Trp and Tyr residues. On cooling after undergoing the thermally induced transition, the enzyme exhibits full enzymatic activity. The lack of protein concentration dependence of the $T_m$ and $\Delta H_{vH}$ for the transition and the invariance in light scattering during the transition demonstrate that no concomitant change in oligomeric structure of the dodecameric protein takes place during unfolding.

The thermal unfolding transition was monitored by changes in Trp exposure to solvent from temperature-induced protein difference spectra and by changes in Tyr exposure from second-derivative spectra. The unfolding reaction involves an increase in exposure of ~0.7 of the 2 Trp/subunit and 2–3 of the 17 Tyr/subunit. In spite of the substantial increase in Tyr exposure, difference spectra showed little perturbation of Tyr because of interference from the Trp perturbation. Thus, second-derivative spectra, which permit determination of absolute Tyr exposure independent of Trp content (Ragone et al., 1984), were used to monitor temperature-induced Tyr perturbations for the $Mn^{2+}$– and $Mg^{2+}$–enzymes and demonstrate a *partially* unfolded final state containing 6.6–7.7 exposed Tyr/subunit as compared to the native folded form with 4.7 Tyr/subunit exposed. *Partial* unfolding is also in accord with estimates of exposure made from changes in Trp extinction differences at ~294 and ~289 nm. In addition, various ligands are observed to bind to the high-temperature form of the enzyme.

The Trp and Tyr perturbations used to monitor the partial unfolding reaction involve a substantial portion of the total Trp and Tyr present, ~35% and ~12%, respectively. This suggests that the thermal transitions are reactions involving true macroscopic states rather than a small number of microstates not representative of the entire enzyme population.

The addition of substrates to the Mn·enzyme increases $T_m$, which was determined from fitting changes in Trp exposure data with a simple two-state model for partial unfolding; this indicates a more negative free energy of ligand binding to the native, folded species than to partially unfolded Mn·enzyme at the concentrations used. However, $Mn^{2+}$ clearly binds to both the native and partially unfolded species as the plot of the free energy of $Mn^{2+}$ binding to native glutamine synthetase vs $1/T_m$ demonstrates by the dramatic change in the sign of the slope from negative to positive in going from low to high free $Mn^{2+}$ concentration (Figure 6). The high-temperature species has more $Mn^{2+}$ binding sites, but the average affinity (on a per binding site basis) is less than that of the low-temperature species. The divalent cation free enzyme undergoes no thermally induced unfolding in the temperature range studied, 2–50 °C, presumably because the protein has already undergone partial unfolding. ADP appears to bind to the partially unfolded Mn·enzyme: (1) the increase in $T_m$ on adding ADP is less than anticipated in view of the affinity of native enzyme for ADP; (2) the increase in Trp exposure to solvent on unfolding is about half that observed with Mn·enzyme in the absence of ADP due to increased Trp burial in the high-temperature form. ADP binds to native glutamine synthetase through bound divalent cation at $n_2$ metal ion sites, and presumably this is also true in the unfolded form. Since the $T_m$ is independent of a 40-fold difference in hydroxylamine concentration in the presence of L-glutamine, the net free energy of hydroxylamine binding to the native and partially unfolded Mn·enzyme is the same under these conditions. L-Glutamine may also bind with low affinity to the partially unfolded Mn·enzyme since L-glutamine interacts weakly with the apoenzyme (Hunt et al., 1975). However, the addition of 150 mM L-glutamine to the Mn·enzyme increases $T_m$ by ~10 °C, and the additional presence of 0.15 mM free ADP causes a total increase of ~19 °C whereas the $T_m$ increases by only ~5 °C in the presence of ADP. This reflects the increased affinity of the native (folded) enzyme for $Mn^{2+}$, L-glutamine, and ADP due to synergistic effects (Shrake et al., 1977; Hunt et al., 1975).

No temperature-induced partial unfolding of the transition-state analogue complex [ADP·$Mn_2$·GS·L-Met-(*S*)-sulfoximine phosphate] is observed up to 72 °C. The extremely negative free energies of binding ADP [$\Delta G' = -17$ kcal/mol (Mauirzi & Ginsburg, 1982a)] and L-Met-(*S*)-sulfoximine phosphate [$\Delta G' \simeq -26$ kcal/mol (Ginsburg et al., 1987)] to native Mn·enzyme more than likely increase $T_m$ beyond 72 °C. The Arrhenius plot of $Mn^{2+}$-supported γ-glutamyl transfer is linear from 4 to 72 °C, and nonlinearity in a van't Hoff plot for $K_m$ for L-glutamine for γ-glutamyl transfer over the same temperature range can be explained with a single temperature-dependent van't Hoff enthalpy for L-glutamine binding to native glutamine synthetase under assay conditions. The native enzyme saturated with substrates also has a $T_m$ above 72 °C, and, consequently, the catalytic activity of the partially unfolded enzyme could not be determined.

At a given free $Mn^{2+}$ concentration, the temperature of half-completion for the partial unfolding of the enzyme determined from changes in Tyr exposure is always higher than that obtained from changes in Trp exposure. The persistent difference between the temperatures of half-completion, i.e., the absence of the tendency to coalesce, as the $Mn^{2+}$ concentration approaches saturation with respect to the native enzyme indicates that this biphasic unfolding process does *not* derive from ligand redistribution during unfolding as previously demonstrated for human albumin (Shrake & Ross, 1988).

The overall partial unfolding of Mn·enzyme ($F \rightleftharpoons U$) appears to involve the unfolding of 2 different, mutually exclusive domains within the protein, one containing at least 1 of the 2 Trp/subunit and the other containing at least 2–3 of the 17 Tyr/subunit, since the temperatures of half-completion for the two, separately monitored transitions are different. By assuming independent Trp and Tyr transitions (random model), the $T_m$ for the partial unfolding of the Mn·enzyme determined from changes in Tyr exposure is consistently 2–3 °C higher than that obtained from changes in Trp exposure at any given free $Mn^{2+}$ concentration. The apparent constant difference at all levels of $Mn^{2+}$ between $T_m$ values for the Trp and Tyr transitions calculated from the random model suggests that in fact the two domains may interact such that any stabilization or destabilization of one domain is reflected in the other. As an extreme form of domain interaction, we have applied a rigorous sequential model for unfolding the two domains with each domain undergoing a two-state unfolding process and with the Trp domain unfolding first. The values of the two transition temperatures are very similar at each $Mn^{2+}$ concentration and show maximum thermal stabilization of the Mn·enzyme at 49 μM free $Mn^{2+}$. On the basis of the fit of the data alone, discriminating between the random and sequential models is not possible. However, the observed correlation between the $T_m$ values for the Trp and Tyr transitions with both models is more easily explained by the sequential model in which there is linkage between the two transitions.

The two domains are mutually exclusive; these cooperative units for the Trp and Tyr unfolding reactions are probably different portions of the subunit rather than the dodecamer in view of the magnitudes of the $\Delta H_{vH}$ values. The two domains may unfold either independently or sequentially with the Trp domain unfolding first. Sequential unfolding (eq 12a) involves a single intermediate (I) whereas independent unfolding (eq 12b) requires two intermediates (I and I′) where intermediate I represents a protein species with the Trp domain unfolded and the Tyr domain folded and intermediate I′ is the converse of I. Independent unfolding of the two domains (eq 12b) requires that $T_m$ and $\Delta H_{vH}$ for the two unfolding reac-

$$F \rightleftharpoons I \rightleftharpoons U \quad (12a)$$

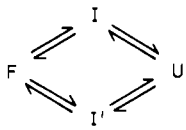


(12b)

tions of the Trp domain ($F \rightleftharpoons I$ and $I' \rightleftharpoons U$) be equal although $\Delta\epsilon^{max}$ values need not be; the same is true for the two-state unfolding reactions of the Tyr domain ($F \rightleftharpoons I'$ and $I \rightleftharpoons U$). Intermediates (I and/or I') are indicated in the second-derivative absorption spectra which show better defined isosbestic points for changes in Trp exposure alone (above 290 nm) than for changes in both Trp and Tyr exposure (below 290 nm) (Figure 5A).

Possible regions of the enzyme subunit involved in the temperature-induced partial unfolding reactions may be identified by means of the X-ray crystallographic data of Almassy et al. (1986). An unusual feature of the enzyme structure is the formation of 12 active sites at heterologous interfaces between subunits within a hexagonal ring of the two face-to-face eclipsed rings. Our results suggest that active-site structures are made more accessible to solvent by increasing temperature. One surface of the active site is formed mainly by six $\beta$-strands of the large C-domain of one subunit and the other by two $\beta$-strands from the Trp-57 loop of the smaller N-terminal domain of the adjacent subunit in a ring of six (Almassy et al., 1986). The two $Mn^{2+}$ binding sites at each active site (Hunt et al., 1975; Hunt & Ginsburg, 1980) as well as the L-glutamate/L-glutamine binding site are in the large C-terminal domain (Almassy et al., 1986), whereas the nucleotide spans the N- and C-domains of adjacent subunits from Lys-47, which can be specifically labeled by the ATP analogue 5'-[*p*-(fluorosulfonyl)benzoyl]adenosine (Pinkofsky et al., 1984), to the $n_2$ divalent cation site. Lys-47 is near the Trp-57 loop, and Trp-57 is only 6 Å from Tyr-397 in the C-domain of the neighboring subunit, which is the site of adenylylation (Almassy et al., 1986). Since there is substantial flexibility in the N-terminal domain (Almassy et al., 1986; David Eisenberg, personal communication), Trp-57 rather than Trp-158 is more than likely the Trp residue exposed during heating. Also, ADP binding appeared to restrict the extent of Trp exposure (Table I); this is consistent with a thermal perturbation of Trp-57. Trp-158 is involved in the formation of central loop structures that interact with identical structures from subunits in the opposite ring (Almassy et al., 1986). Possibly Trp-158 becomes partially exposed during the removal of $Mn^{2+}$ or $Mg^{2+}$ from the enzyme since such treatment destabilizes quaternary structures (Ginsburg, 1972).

Tyr residues that are exposed during heating can be assigned to the subunit C-terminal domain since none are in the N-terminal domain. Tyr-179, -296, and -397 are among the highly mobile Tyr residues near the active site and have large X-ray temperature factors (David Eisenberg, personal communication). However, identification of the two to three Tyr residues that are exposed during heating currently is not possible. For example, Tyr-397 is near the surface and is already exposed for enzyme-catalyzed adenylylation (Almassy et al., 1986). This residue also appeared to be buried during the binding of the L-glutamate analogue L-Met-(*SR*)-sulfoximine, which makes the unadenylylated enzyme more compact (Shrake et al., 1980; Hunt & Ginsburg, 1980). Even though there is uncertainty in the assignment of thermally exposed Tyr residues, these residues are in a different subunit domain than is Trp-57, and this justifies our conclusion that Tyr and Trp exposure during heating occurs in two separate domains. The location of the Tyr residue in the C-domain is unclear. Almassy et al. (1986) remark that removal of divalent metal ions from the enzyme would be expected to exert a disorienting influence on the eight $\beta$-strands around the active site. Likewise, heating also could perturb structures forming the active sites.

In summary, reversible thermal transitions studied here appear to involve alterations of active-site structures in both the N- and C-terminal domains near heterologous contacts between intra-ring subunits in the glutamine synthetase dodecamer. The thermally induced Tyr and Trp exposure may reflect rather long-range effects on the orientation of eight $\beta$-strands forming the active site [see Almassy et al. (1986)]. By monitoring both Trp and Tyr exposure during heating, the independent unfolding of two different subunit domains was detected.

**Registry No.** GS, 9023-70-5; L-*S*-MetSox, 21752-32-9; L-*R*-MetSox, 21752-31-8; ADP, 58-64-0; L-Gln, 56-85-9; L-*S*-MSoxP, 109528-34-9; L-*R*-MSoxP, 121192-77-6; Mn, 7439-96-5; $NH_2OH$, 7803-49-8.

## References


Almassy, R. J., Janson, C. A., Hamlin, R., Xuong, N.-H., & Eisenberg, D. (1986) *Nature (London) 323*, 304–309.

Baldwin, R. L. (1986) *Proc. Natl. Acad. Sci. U.S.A. 83*, 8069–8072.

Brandts, J. F. (1964) *J. Am. Chem. Soc. 86*, 4302–4314.

Caban, E. C., & Ginsburg, A. (1976) *Biochemistry 15*, 1569–1580.

Colombo, G., & Villafranca, J. J. (1986) *J. Biol. Chem. 261*, 10587–10591.

Demchenko, A. P. (1986) *Ultraviolet Spectroscopy*, p 110, Springer-Verlag, Berlin.

Denton, M. D., & Ginsburg, A. (1969) *Biochemistry 8*, 1714–1725.

Edge, V., Allewell, N. M., & Sturtevant, J. M. (1985) *Biochemistry 24*, 5899–5906.

Gass, J. D., & Meister, A. (1970) *Biochemistry 9*, 1380–1390.

Ginsburg, A. (1972) *Adv. Protein Chem. 26*, 1–79.

Ginsburg, A., Yeh, J., Henning, S. B., & Denton, M. D. (1970) *Biochemistry 9*, 633–649.

Ginsburg, A., Gorman, E. G., Neece, S. H., & Blackburn, M. B. (1987) *Biochemistry 26*, 5989–5996.

Gorman, E. G., & Ginsburg, A. (1982) *J. Biol. Chem. 257*, 8244–8252.

Hunt, J. B., & Ginsburg, A. (1972) *Biochemistry 11*, 3723–3735.

Hunt, J. B., & Ginsburg, A. (1980) *J. Biol. Chem. 255*, 590–594.

Hunt, J. B., Smyrniotis, P. Z., Ginsburg, A., & Stadtman, E. R. (1975) *Arch. Biochem. Biophys. 166*, 102–124.

Kauzmann, W. (1959) *Adv. Protein Chem. 14*, 1–63.

Kauzmann, W. (1987) *Nature (London) 325*, 763–764.

Leach, S. J., & Smith, J. A. (1972) *Int. J. Protein Res. 4*, 11–19.

Lumry, R., Biltonen, R. L., & Brandts, J. F. (1966) *Biopolymers 4*, 917–944.

Manley, S. P., Matthews, K. S., & Sturtevant, J. M. (1985) *Biochemistry 24*, 3842–3846.

Maurizi, M. R., & Ginsburg, A. (1982a) *J. Biol. Chem. 257*, 4271–4278.

Maurizi, M. R., & Ginsburg, A. (1982b) *J. Biol. Chem. 257*, 7246–7251.

Maurizi, M. R., & Ginsburg, A. (1986) *Biochemistry 25*, 131–140.

Meister, A. (1974) *Enzymes (3rd Ed.) 10*, 699–754.

Noggle, J. H. (1985) *F-Curve*, LEDS Publishing Co., Research Triangle Park, NC.
Pace, N. (1975) *CRC Crit. Rev. Biochem. 2*, 1-43.
Pinkofsky, H. B., Ginsburg, A., Reardon, I., & Heinrikson, R. L. (1984) *J. Biol. Chem. 259*, 9616-9622.
Privalov, P. L. (1979) *Adv. Protein Chem. 33*, 167-241.
Privalov, P. L. (1982) *Adv. Protein Chem. 35*, 1-104.
Ragone, R., Colonna, G., Balestrieri, C., Servillo, L., & Irace, G. (1984) *Biochemistry 23*, 1871-1875.
Ragone, R., Colonna, G., Bismuto, E., & Irace, G. (1987) *Biochemistry 26*, 2130-2134.
Sãnchez-Ruiz, J. M., Lõpez-Lacomba, J. L., Cortijo, M., & Mateo, P. L. (1988) *Biochemistry 27*, 1648-1652.
Schellman, J. A. (1975) *Biopolymers 14*, 999-1018.
Schellman, J. A. (1976) *Biopolymers 15*, 999-1000.
Schellman, J. A. (1987a) *Annu. Rev. Biophys. Biophys. Chem. 16*, 115-137.
Schellman, J. A. (1987b) *Biopolymers 26*, 549-559.
Shapiro, B. M., & Ginsburg, A. (1968) *Biochemistry 7*, 2153-2167.
Shortle, D. (1987) in *Protein Structure, Folding, and Design*, pp 353-361, Alan R. Liss, New York.
Shrake, A., & Rupley, J. K. (1980) *Biochemistry 19*, 4044-4051.
Shrake, A., & Ross, P. D. (1988) *J. Biol. Chem. 263*, 15392-15399.
Shrake, A., Powers, D. M., & Ginsburg, A. (1977) *Biochemistry 16*, 4372-4381.
Shrake, A., Whitley, E. J., Jr., & Ginsburg, A. (1980) *J. Biol. Chem. 255*, 581-589.
Shrake, A., Ginsburg, A., Wedler, F. C., & Sugiyama, Y. (1982) *J. Biol. Chem. 257*, 8238-8243.
Shrake, A., McFarland, P. J., Fisher, M. T., & Ginsburg, A. (1988) *Biophys. J. 53*, 292a.
Stadtman, E. R., & Ginsburg, A. (1974) *Enzymes (3rd Ed.) 10*, 755-807.
Stadtman, E. R. Smyrniotis, P. Z., Davis, J. N., & Wittenberger, M. E. (1979) *Anal. Biochem. 95*, 275-285.
Sturtevant, J. M. (1977) *Proc. Natl. Acad. Sci. U.S.A. 74*, 2236-2240.
Woolfolk, C. A., Shapiro, B. M., & Stadtman, E. R. (1966) *Arch. Biochem. Biophys. 116*, 177-192.

# Phosphonate Analogues of Carboxypeptidase A Substrates Are Potent Transition-State Analogue Inhibitors†

John E. Hanson, Alan P. Kaplan, and Paul A. Bartlett*
*Department of Chemistry, University of California, Berkeley, California 94720*
*Received December 19, 1988; Revised Manuscript Received March 10, 1989*

ABSTRACT: Analogues of tri- and tetrapeptide substrates of carboxypeptidase A in which the scissile peptide linkage is replaced with a phosphonate moiety ($-PO_2^-$–O–) were synthesized and evaluated as inhibitors of the enzyme. The inhibitors terminated with either L-lactate or L-phenyllactate [designated (O)Ala and (O)Phe, respectively] in the $P_1'$ position. Transition-state analogy was shown for a series of 14 tri- and tetrapeptide derivatives containing the structure RCO-Ala$^P$-(O)Ala [RCO-A$^P$(O)A, A$^P$ indicates the phosphonic acid analogue of alanine] by the correlation of the $K_i$ values for the inhibitors and the $K_m/k_{cat}$ values for the corresponding amide substrates. This correlation supports a transition state for the enzymatic reaction that resembles the tetrahedral intermediate formed upon addition of water to the scissile carbonyl group. The inhibitors containing (O)Phe at the $P_1'$ position proved to be the most potent reversible inhibitors of carboxypeptidase A reported to date: the dissociation constants of ZAF$^P$(O)F, ZAA$^P$(O)F, and ZFA$^P$(O)F are 4, 3, and 1 pM, respectively. Because of the high affinity of these inhibitors, their dissociation constants could not be determined by steady-state methods. Instead, the course of the association and dissociation processes was monitored for each inhibitor as its equilibrium with the enzyme was established in both the forward and reverse directions. A phosphonamidate analogue, ZAA$^P$F, in which the peptide linkage is replaced with a $-PO_2^-$–NH– moiety, was prepared and shown to hydrolyze rapidly at neutral pH ($t_{1/2}$ = 20 min at pH 7.5). This inhibitor is bound an order of magnitude *less* tightly than the corresponding phosphonate, ZAA$^P$(O)F, a result that contrasts with the 840-fold higher affinity of phosphonamidates for thermolysin [Bartlett, P. A., & Marlowe, C. K. (1987) *Science 235*, 569-571], a zinc peptidase with a similar arrangement of active-site catalytic residues.

Substrate analogues in which the scissile peptide linkage is replaced with a tetrahedral phosphorus ester or amide moiety are potent inhibitors of zinc peptidases (Komiyama et al., 1975; Weaver et al., 1977; Kam et al., 1979; Nishino & Powers, 1979; Hoffmann & Rottenberg, 1980; Jacobsen & Bartlett, 1981a,b; Thorsett et al., 1982; Bartlett & Marlowe, 1983, 1987a,b; Galardy et al., 1983; Grobelny et al., 1985a; Yamauchi et al., 1985; Mookthiar et al., 1987; Karanewsky et al., 1988). The basis for this inhibition is attributed to the similarity of the tetrahedral phosphorus species to the presumed tetrahedral intermediate arising from addition of a zinc-bound water molecule to the substrate carbonyl group (Tronrud et al., 1970; Nishino & Powers, 1979). There is both thermodynamic as well as structural evidence in support of this concept. For thermolysin (TLN), the $K_i$ values for a series of phosphonamidate tripeptide inhibitors show a strong cor-

†Support for this research was provided by a National Science Foundation Predoctoral Fellowship to J.E.H. and a grant (CA-22747) to P.A.B. from the National Institutes of Health.

0006-2960/89/0428-6294$01.50/0 © 1989 American Chemical Society